Electrostatics in Liquids

Salvatore Assenza

September 26, 2024

1 Introduction

This chapter considers the so-called electrostatic interactions, which involve the presence of ions in the solution. Technically speaking, also the van der Waals interactions are ultimately electrostatic in nature, but in that case overall neutral molecules are considered, which interact universally via their (induced) dipole moments. It is customary in biophysics to call "electrostatic interactions" only the ones involving objects with a net charge, such as the systems that we will study here. The sources of this material are mainly the two references that are listed at the end of the document. In addition, it is worth acknowledging M. Rubinstein for various scaling computations reported below, which he presented in a class given in 2012 at the Boulder Summer School on Polymers in Soft and Biological Matter.

2 Poisson-Boltzmann Equation

Ions in solution are free to diffuse. Hence, a positive ion finds itself at the center of a competition between an enthalpic term, which pushes to localize it around negative charges, and its translational entropy. Naturally, the same applies for negative ions, which tend to be localized around positive charges but also have translational entropy. In biophysics, there are a lot of charged objects: free simple ions in solution (e.g. Na^+ or Cl^-); proteins; DNA; membrane lipids. In order to understand the behavior of a biophysical system, it is hence of the utmost importance to be capable of describing the way in which these agents interact with each other.

In order to start our discussion on electrostatics in liquids, let us assume for simplicity that we have a set of monovalent charges $\pm e_0 = \pm 1.6 \cdot 10^{-19}$ C with average number density ρ_0. Their concentration in molarity (1 M = 1 mol/l) is often called the *ionic strength* I of the solution, and is related to the number density via the formula $I = 10^3 \rho_0 / N_A$, where $N_A = 6.022 \cdot 10^{23}$ mol^{-1} is Avogadro's constant. Quite often, one uses as unit measure 1 mM $= 10^{-3}$ mol/l $= 1$ mol/m^3. In this case, $I = \rho_0 / N_A$.

Our goal is to compute the total electrostatic potential ψ in the vicinity of an arbitrarily selected charge $\overline{q}$, which we fix as being positive to clarify the discussion. Very close to the charge, we expect ψ to be practically equal to the standard Coulomb potential. In contrast, at larger distances the other free charges will come into play. From a qualitative point of view, it is expected that in the vicinity of $\overline{q}$ one finds more negative than positive charges, due to the electrostatic interaction with $\overline{q}$. Hence, the potential generated by this cloud of charges has opposite sign than the one generated by $\overline{q}$, so that we expect that the resulting overall potential is weaker than the standard Coulomb formula, i.e. that it is *screened*. We also expect a dependence on I: the larger the concentration of charges, the more the charges in the cloud, which results into a stronger screening. Finally, it is desirable that the potential reduces to the Coulomb one in the limit $I \to 0$.

Now, one of Maxwell equations (corresponding to Gauss' law) is the so-called *Poisson equation*, which relates the electrostatic potential ψ to the source provided by the charges $e_0 \rho_+$ and $-e_0 \rho_-$:

$$\nabla^2 \psi = -\frac{e_0 \rho_+}{\epsilon_0 \epsilon} + \frac{e_0 \rho_-}{\epsilon_0 \epsilon} = -\frac{e_0}{\epsilon_0 \epsilon} \left(\rho_+ - \rho_- \right) \ . \tag{1}$$

Note that we are considering different, space-dependent ρ_+ and ρ_- to account for the presence of clouds around $\overline{q}$. We expect that $\rho_+, \rho_- \simeq \rho_0$ at large distances.

On the other hand, at thermodynamic equilibrium the concentrations follow the Boltzmann distribution. The energy is provided by the electrostatic interaction and is equal to $\pm e_0 \psi$ according to the sign of the charges considered. Since it is reasonable that $\psi \to 0$ at large distances, we can write

$$\rho_+ = \rho_0 e^{-\frac{e_0 \psi}{k_B T}} \qquad \text{and} \qquad \rho_- = \rho_0 e^{\frac{e_0 \psi}{k_B T}} \ . \tag{2}$$

Joining this formula with Poisson's equation, we thus obtain

$$\nabla^2\psi = -\frac{e_0\rho_0}{\epsilon_0\epsilon}\left(e^{-\frac{e_0\psi}{k_BT}} - e^{\frac{e_0\psi}{k_BT}}\right) . \tag{3}$$

This formula, which for pretty obvious reasons is called *Poisson-Boltzmann's equation*, provides a second-order differential equation from which to determine the electrostatic potential ψ.

Due to its high non-linearity, it can be solved exactly only in a few cases. However, for $e_0\psi/(k_BT) \ll 1$ (corresponding to $\psi \ll 26$ mV at $T = 300$ K) one can linearize the Poisson-Boltzmann equation and obtain

$$\nabla^2\psi \simeq -\frac{e_0\rho_0}{\epsilon_0\epsilon}\left(1 - \frac{e_0\psi}{k_BT} - 1 - \frac{e_0\psi}{k_BT}\right) = \frac{2e_0^2\rho_0}{\epsilon_0\epsilon k_BT}\psi . \tag{4}$$

The linearized version of the Poisson-Boltzmann equation is called the *Debye-Hückel equation*. The numerical factor has the units of the square of an inverse length. Thus, we define the *Debye length* l_D as

$$l_D \equiv \sqrt{\frac{\epsilon_0\epsilon k_BT}{2e_0^2\rho_0}} . \tag{5}$$

In this way, the Debye-Hückel equation can be written as

$$\nabla^2\psi = \frac{1}{l_D^2}\psi . \tag{6}$$

Before proceeding further, it is useful to define another constant l_B, called the *Bjerrum length*, which corresponds to the distance at which two elementary charges have a Coulomb interaction energy equal to k_BT. Hence, by definition

$$l_B \equiv \frac{e_0^2}{4\pi\epsilon_0\epsilon k_BT} . \tag{7}$$

The Bjerrum length of water at room temperature ($\epsilon \simeq 78, T = 300$ K) is $l_B \simeq 0.7$ nm. Using the Bjerrum length, and remembering that $\rho_0 = N_AI$, we can rewrite the Debye length as

$$l_D = \frac{1}{\sqrt{8\pi l_B\rho_0}} = \frac{1}{\sqrt{8\pi l_B N_A I}} \quad (I \text{ in mM}). \tag{8}$$

At physiological conditions, one has typically $I \simeq 150$ mM, which results into $l_D \simeq 0.8$ nm, which is numerically close to l_B. We will analyze further l_D once we solve the Debye-Hückel equation for a free ion.

3 Potential generated by a free ion

We now aim to solve the Debye-Hückel equation for a free ion. Considering a reference system with origin at the ion, we note that the system has a spherical symmetry, i.e. $\psi(\boldsymbol{r}) = \psi(r)$. As a consequence, the Laplacian operator $\nabla^2 = \frac{d^2}{dx^2} + \frac{d^2}{dy^2} + \frac{d^2}{dz^2}$ can be written in terms of just the polar distance r, obtaining

$$\nabla^2\psi = \frac{1}{r^2}\frac{d}{dr}\left(r^2\frac{d\psi}{dr}\right) = \frac{1}{l_D^2}\psi \ . \tag{9}$$

This one-dimensional differential equation can be solved by defining an auxiliary function $u \equiv r\psi$, so that

$$\begin{cases} \psi = \frac{u}{r} \\ \frac{d\psi}{dr} = \frac{1}{r}\frac{du}{dr} - \frac{u}{r^2} \\ \frac{d^2\psi}{dr^2} = \frac{1}{r}\frac{d^2u}{dr^2} - \frac{2}{r^2}\frac{du}{dr} + \frac{2u}{r^3} \end{cases} \tag{10}$$

Developing the derivatives in Eq.(9) and substituting, the equation becomes

$$\frac{d^2u}{dr^2} = \frac{1}{l_D^2}u \ . \tag{11}$$

This equation can be solved directly, giving

$$u = A\, e^{\frac{r}{l_D}} + B\, e^{-\frac{r}{l_D}} \ , \tag{12}$$

where A and B are constants to be determined from the boundary conditions. Before doing so, we write explicitly the potential as

$$\psi = A\,\frac{e^{\frac{r}{l_D}}}{r} + B\,\frac{e^{-\frac{r}{l_D}}}{r} \ . \tag{13}$$

Now, the potential at infinite distance has to go to zero, so that the exponential with a positive exponent is not a physically-acceptable solution, i.e. $A = 0$. Moreover, we want to retrieve Coulomb's law when the ionic strength vanishes. In the limit $I \to 0$, from Eq.(8) we get $l_D \to \infty \Rightarrow e^{-r/l_D} \to 1$. Hence, in this limit $\psi = A/r = e_0/(4\pi\epsilon_0\epsilon r) \Rightarrow A = e_0/(4\pi\epsilon_0\epsilon)$. Summarizing, we obtain the *Debye-Hückel formula* for the potential generated by a free ion:

$$\psi(r) = \frac{e_0}{4\pi\epsilon_0\epsilon r}e^{-\frac{r}{l_D}} \ . \tag{14}$$

This formula tells us that the potential behaves as the standard Coulomb law with an exponentially-decaying screening factor. Now, let us consider the interaction free energies of positive and negative ions. First of all a bit of nomenclature: ions with equal charge as the reference ion are called *coions*, while oppositely-charged ions are called *counterions*. In the present case, the

reference ion is positive, so that the coions are the positive charges and the counterions the negative ones. The corresponding free energies of interaction are

$$F_+(r) = e_0\psi(r) = \frac{e_0^2}{4\pi\epsilon_0\epsilon r}e^{-\frac{r}{l_D}} \qquad \text{and} \qquad F_-(r) = -e_0\psi(r) = -\frac{e_0^2}{4\pi\epsilon_0\epsilon r}e^{-\frac{r}{l_D}}\ , \tag{15}$$

respectively. The potential ψ and the repulsive energy $F_+(r)$ are plotted in Fig.1a for two values of ionic strength, namely $I = 10$ mM (orange dashed line) and $I = 150$ mM (green dotted line). As expected, larger values of I correspond to stronger screening (i.e., lower values of both the potential and the interaction energy), and in all cases the interaction is weaker than a pure Coulomb interaction (blue continuous line). The corresponding charge densities are obtained as

$$\rho_+(r) = \rho_0\, e^{-\frac{e_0\psi(r)}{k_BT}} = \rho_0\, e^{-\frac{e_0^2}{4\pi\epsilon_0\epsilon k_BTr}e^{-\frac{r}{l_D}}} \qquad \text{and} \qquad \rho_-(r) = \rho_0\, e^{\frac{e_0\psi(r)}{k_BT}} = \rho_0\, e^{\frac{e_0^2}{4\pi\epsilon_0\epsilon k_BTr}e^{-\frac{r}{l_D}}}\ , \tag{16}$$

respectively, and are plotted in Fig.1b for $I = 150$ mM. The plot clearly shows the unequal distribution of coions (blue continuous line) and counterions (yellow dashed line) in close proximity of the reference ion, with the counterions being more present than in bulk (horizontal line). This excess (or lack) of charges is eliminated at large distances, where both ρ_+ and ρ_- approach the bulk value ρ_0.

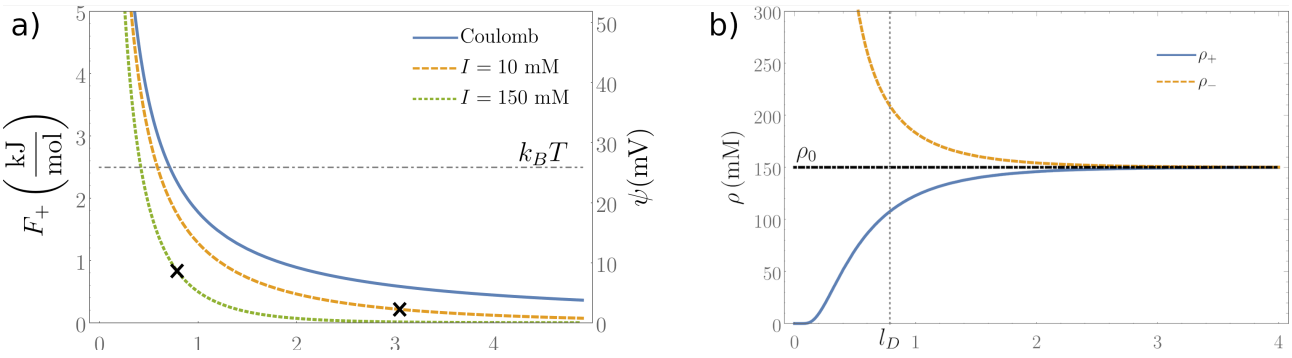

Figure 1: a) Debye-Hückel repulsive energy between two monovalent ions (left axis, Eq.(15)) and corresponding potential (right axis, Eq.(14)) as a function of distance for $I = 10$ mM (orange dashed line) and $I = 150$ mM (green dotted line). For comparison, the corresponding Coulomb function is plotted as a blue continuous line, while the thermal energy k_BT is drawn as a horizontal line. The marked points correspond to the Debye length for each case. b) Ion density for $I = 150$ mM in the vicinity of a reference ion with positive charge, plotted for positive (blue continuous line) and negative (dashed orange line) charges. The bulk density $\rho_0 = 150$ mM is reported as an horizontal line. The Debye length is indicated by a vertical line.

3.1 The Debye Length

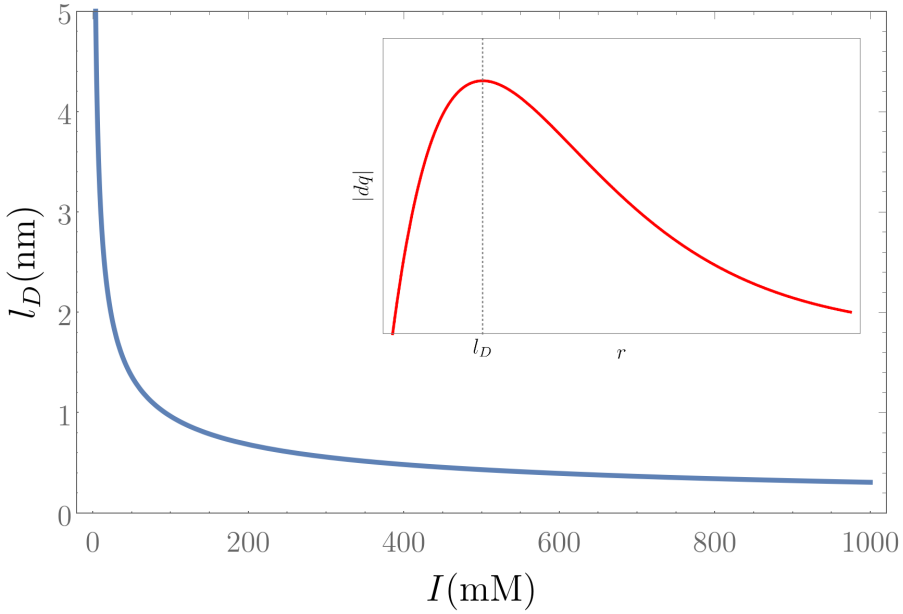

Figure 2: Dependence of the Debye length l_D on the ionic strength I of the solution. In the inset, we plot the magnitude of the charge found in a spherical shell at distance r from the reference ion. The vertical line corresponds to $r = l_D$.

Eq.(14) enables a physical interpretation of the Debye length as the length scale of the exponential decay of the electrostatic screening imposed by the cloud of nearby ions. As seen in Eq.(5), $l_D \propto 1/\sqrt{I}$, so that larger concentrations of ions will correspond to lower values of l_D, i.e. faster decay. This makes sense, since for larger concentrations we expect a stronger screening effect. The Debye length is plotted as a function of I in Fig.2.

In order to better grasp the physical meaning of l_D, it is useful to make some considerations. Particularly, in order to characterize the cloud of ions, we proceed to compute the total infinitesimal charge $dq(r)$ found within a spherical shell at distance r from the reference ion. The charge density $e_0(\rho_+ - \rho_-)$ at distance r is regulated by Eq.(16). The infinitesimal charge $dq(r)$ is found by integrating the charge density over the polar angles, hence yielding

$$dq(r) = e_0(\rho_+ - \rho_-) \cdot 4\pi r^2 dr \ . \tag{17}$$

Substitution from Eq.(16) gives

$$dq(r) = 4\pi r^2 e_0 \rho_0 \left(e^{-\frac{e_0\psi}{k_B T}} - e^{\frac{e_0\psi}{k_B T}} \right) dr = -8\pi r^2 e_0 \rho_0 \sinh\left(\frac{e_0\psi}{k_B T} \right) dr \ . \tag{18}$$

In the spirit of the Debye-Hückel approximation, we consider the potential to be small, i.e. $\psi \ll k_B T/e_0 \simeq 26$ mV. This is certainly correct at large enough distances, although this

approximation breaks down at low values of r, as can be seen from Fig.1a. For what comes, we need it to hold around $r \simeq l_D$, which correspond to the marked points in Fig.1a and are fairly below the threshold value indicated by the horizontal line. If $\psi \ll k_B T/e_0$, we can write

$$dq(r) \simeq -8\pi r^2 e_0 \rho_0 \cdot \frac{e_0 \psi}{k_B T} \cdot dr = -8\pi r^2 e_0 \rho_0 \cdot \frac{e_0}{k_B T} \cdot \frac{e_0}{4\pi\epsilon_0 \epsilon r} e^{-\frac{r}{l_D}} \cdot dr \ , \tag{19}$$

where we have substituted Eq.(14). From the definition of the Bjerrum length, Eq.(7), we can write

$$dq(r) \simeq -8\pi r e_0 \rho_0 l_B e^{-\frac{r}{l_D}} \cdot dr \propto -r e^{-\frac{r}{l_D}} \ , \tag{20}$$

The negative sign of dq indicates that there is an excess of counterions (here corresponding to negative charges), induced by the electrostatic attraction and in agreement with Fig.1b. As for its magnitude, which is represented in the inset of Fig.2, it shows a peak for $r = l_D$. This provides an intuitive understanding of the Debye length, as being the distance at which there is the largest concentration of counterions. Hence, the system can be imagined as having on average each ion surrounded by a cloud of counterions of size l_D.

Problem. As mentioned above, the interaction energies $F_\pm(r)$ reported in Eq.(15) are free energies, since they include the effect of the translational entropy of ions. Starting from Eq.(15) and using the Maxwell relation $S = -\partial F/\partial T$, show that the enthalpic and entropic contributions are

$$U = F\left(1 - \frac{r}{2l_D}\right) \qquad \text{and} \qquad -TS = F \cdot \frac{r}{2l_D} \ , \tag{21}$$

respectively. Plot the ratios $|-TS/F|$ and $|U/F|$ as a function of r. Which contribution leads the interaction at small r? Which is more important at large r?

3.1.1 A scaling argument

This physical picture can also be supported by a scaling argument (hence no numerical prefactors are considered) Let us consider for the entropy the simple case of an ideal gas, and let us consider a certain region of size R within the system (no reference ions are present in this study). The corresponding volume scales as $V_R \sim R^3$. Since the bulk concentration is ρ_0, and we are neglecting the effect of the electrostatic interaction on the distribution of ions, the average number of ions within V_R is

$$\langle n_+ \rangle = \langle n_- \rangle \sim \rho_0 V_R \sim \rho_0 R^3 \ . \tag{22}$$

The electrostatic energy within the system can be roughly estimated as

$$U_e \sim \frac{Q^2}{\epsilon_0 \epsilon R} \ , \tag{23}$$

where $Q = e_0(n_+ - n_-)$ is the total charge found therein. Now, on average the total charge in the region is $< Q >= e_0(< n_+ > - < n_- >) = 0$. However, the electrostatic energy goes quadratically with Q, so that its average will be driven by fluctuations:

$$\langle U_e \rangle \sim \frac{\langle Q^2 \rangle}{\epsilon_0 \epsilon R} \sim \frac{e_0^2 \left\langle (n_+ - n_-)^2 \right\rangle}{\epsilon_0 \epsilon R} \, . \tag{24}$$

In an ideal gas, it can be shown that the fluctuations scale with the size of the system[1], i.e. $\langle \Delta n^2 \rangle \equiv \left\langle (n_+ - n_-)^2 \right\rangle >\sim< n_+ >\sim \rho_0 R^3$. This enables writing for the energy

$$\langle U_e \rangle \sim \frac{e_0^2 \rho_0 R^3}{\epsilon_0 \epsilon R} = \frac{e_0^2 \rho_0 R^2}{\epsilon_0 \epsilon} \propto R^2 \, . \tag{25}$$

Therefore, *the electrostatic energy increases with the size of the considered region*, which is expected due to its long range. As a consequence, it is expected that at low length scales the thermal energy $k_B T$ is enough to overcome the electrostatic interaction, while the latter becomes more important at larger scales. A natural question is thus: at which length scale $\overline{R}$ does the crossover take place? The answer is easy to find:

$$\langle U_e \rangle \sim k_B T \Rightarrow \frac{e_0^2 \rho_0 \overline{R}^2}{\epsilon_0 \epsilon} \sim k_B T \Rightarrow \overline{R} \sim \sqrt{\frac{1}{\rho_0 \cdot \frac{e_0^2}{k_B T \epsilon_0 \epsilon}}} \sim \sqrt{\frac{1}{\rho_0 l_B}} \sim l_D \, , \tag{26}$$

where we have used the definitions of Bjerrum and Debye lengths given by Eq.(7) and Eq.(5), respectively. This scaling argument provides an alternative global view of the Debye length (as opposed to the one considered above and focused on a reference ion). Indeed, l_D corresponds to the crossover between the short-scale entropy-dominated regime to the large-scale regime where the electrostatic energy gives the main contribution. Hence, one can think of the whole system as a collection of "blobs" of size l_D such that inside each blob the ions are essentially non-interacting, while blobs are correlated with each other. Hence, inside a blob the fluctuations scale as $\langle \Delta n^2 \rangle \sim \langle n_+ \rangle \propto R^3$, while it is expected that they grow more slowly at large scales. The dependence of fluctuations on size for $R \gg l_D$ can be estimated by observing that the thermal energy is still "pumping" fluctuations that enter in the electrostatic energy via $\langle Q^2 \rangle$. The relation $\langle U_e \rangle \sim k_B T$ is still valid, but now the correlations imposed by the electrostatic energy result in $\langle \Delta n^2 \rangle_{\text{corr}} \ll \langle n_+ \rangle$. Equating electrostatic and thermal energy we obtain

$$\langle U_e \rangle \sim k_B T \Rightarrow \frac{e_0^2 \langle \Delta n^2 \rangle_{\text{corr}}}{\epsilon_0 \epsilon R} \sim k_B T \Rightarrow \left\langle \Delta n^2 \right\rangle_{\text{corr}} \sim \frac{R}{\frac{e_0^2}{k_B T \epsilon_0 \epsilon_r}} \sim \frac{R}{l_B} \propto R \, . \tag{27}$$

The increase of fluctuations with size has slowed down from $\propto R^3$ to $\propto R$. The ratio between the size of fluctuations in the correlated and uncorrelated cases is

$$\frac{\langle \Delta n^2 \rangle_{\text{corr}}}{\langle \Delta n^2 \rangle} \sim \frac{\frac{R}{l_B}}{\rho R^3} = \frac{1}{\rho l_B R^2} \ll 1 \, . \tag{28}$$

[1]For a proof, see the calculation at the end of this section.

Fluctuations scale with the size of the system: a proof.

Let us consider an ideal gas found in two boxes of volume V_1 and $V_2 \gg V_1$ in which it can move freely. If there are n molecules in the first box and N molecules in total, the total number of states is $\Omega(n) \sim V_1^n V_2^{N-n} = (V_1/V_2)^n \cdot V_2^N = x^n V_2^N$, where $x \equiv V_1/V_2 \ll 1$. The partition function can be written as

$$\mathcal{Z} = \sum_{n=0}^{N} \Omega(n) = V_2^N \cdot \sum_{n=0}^{N} x^n = V_2^N \frac{1-x^N}{1-x} \simeq V_2^N \frac{1}{1-x} \,, \tag{29}$$

since $x \ll 1$ and $N \gg 1$. The average number of molecules in the first box is

$$\langle n \rangle = \frac{1}{\mathcal{Z}} \sum_{n=0}^{N} n\Omega(n) = \frac{\sum_{n=0}^{N} nx^n}{\frac{1}{1-x}} \,. \tag{30}$$

The numerator can be computed in the following way:

$$\sum_{n=0}^{N} nx^n = x \sum_{n=0}^{N} nx^{n-1} = x \frac{d}{dx} \sum_{n=0}^{N} x^n = x \frac{d}{dx} \frac{1}{1-x} = \frac{x}{(1-x)^2} \,. \tag{31}$$

Hence,

$$\langle n \rangle = \frac{x}{1-x} \,. \tag{32}$$

The average square number of atoms is

$$\left\langle n^2 \right\rangle = \frac{1}{\mathcal{Z}} \sum_{n=0}^{N} n^2 \Omega(n) = \frac{\sum_{n=0}^{N} n^2 x^n}{\frac{1}{1-x}} \,. \tag{33}$$

Similarly to the previous case, we find for the numerator

$$\sum_{n=0}^{N} n^2 x^n = x \sum_{n=0}^{N} n^2 x^{n-1} = x \frac{d}{dx} \sum_{n=0}^{N} nx^n = \frac{2x^2}{(1-x)^3} \,. \tag{34}$$

Hence,

$$\left\langle n^2 \right\rangle = \frac{x\,(1+x)}{(1-x)^2} \,. \tag{35}$$

The average size of fluctuations is thus ($\langle n \rangle$ is a constant with respect to averaging)

$$\left\langle (n - \langle n \rangle)^2 \right\rangle = \left\langle n^2 \right\rangle - \langle n \rangle^2 = \frac{x\,(1+x)}{(1-x)^2} - \frac{x^2}{(1-x)^2} = \frac{x}{(1-x)^2} = \frac{\langle n \rangle}{1-x} \propto \langle n \rangle \,. \tag{36}$$

4 General electroneutral solution

The calculations reported up to this point have been done under the assumption of a simple solution of monovalent ions, e.g. Na^+ and Cl^-. We now consider the more general case where there is a cocktail of ions of valencies $z_1, z_2, \ldots, z_k$, where z_i can be either positive or negative. The simple case considered above corresponds to $k = 2$, $z_1 = 1$ and $z_2 = -1$. In the systems of interest in biophysics, the presence of ions is typically due to the separation of complexes with overall neutral electric charge. For instance, the dissolution of a salt (such as NaCl), or the release of a positive charge from proteins with carboxylic groups in water: $COOH \rightarrow COO^- + H^+$. Therefore, one usually assumes that the system under study is overall neutral. In this case, if we denote as $\rho_{0,1}, \rho_{0,2} \ldots, \rho_{0,k}$ the bulk concentrations of the various ions, electroneutrality can be expressed as the condition

$$\sum_{i=1}^{k} z_i \rho_{0,i} = 0 \; . \tag{37}$$

Repeating the steps that led to Eq.(3), in the general case we obtain for the Poisson-Boltzmann equation:

$$\nabla^2 \psi = -\frac{e_0}{\epsilon_0 \epsilon} \sum_{i=1}^{k} z_i \rho_{0,i} e^{-\frac{e_0 z_i \psi}{k_B T}} \; . \tag{38}$$

Under the assumption of weak potentials, we can write

$$\nabla^2 \psi \simeq -\frac{e_0}{\epsilon_0 \epsilon} \sum_{i=1}^{k} z_i \rho_{0,i} \left(1 - \frac{e_0 z_i \psi}{k_B T} \right) \; . \tag{39}$$

Due to the electroneutrality condition, the first term in the previous equation is zero, so that

$$\nabla^2 \psi \simeq \left(\sum_{i=1}^{k} \frac{e_0^2 z_i^2 \rho_{0,i}}{k_B T \epsilon_0 \epsilon} \right) \psi = \frac{1}{l_D^2} \psi \; , \tag{40}$$

where we have defined the Debye length as

$$l_D \equiv \sqrt{\frac{k_B T \epsilon_0 \epsilon}{e_0^2 \sum_{i=1}^{k} z_i^2 \rho_{0,i}}} = \frac{1}{\sqrt{4\pi l_B \sum_{i=1}^{k} z_i^2 \rho_{0,i}}} \; . \tag{41}$$

Defininig the ionic strength I as

$$I \equiv \frac{\sum_{i=1}^{k} z_i^2 \rho_{0,i}}{2 N_A} \tag{42}$$

we can write $l_D = 1/\sqrt{8\pi l_B N_A I}$, which is formally equivalent to Eq.(8). We note that for the monovalent case $k = 2$,$z_1 = 1$,$z_2 = -1$ and $\rho_{0,1} = \rho_{0,2} = \rho_0$ so that $I = 2\rho_0/(2N_A) = \rho_0/N_A$,

which is coherent with the definition given above. Therefore, we conclude that within the Debye-Hückel approximation the presence of different ions only affects the way in which the ionic strength is computed, while the formulas are practically the same. One has only to be careful in including the valencies where needed. For instance, the valency z^* of the reference ion has to be inserted in the potential, so that Eq.(14) now becomes

$$\psi(r) = \frac{z^* e_0}{4\pi\epsilon_0\epsilon r} e^{-\frac{r}{l_D}} \ . \tag{43}$$

Similarly, the interaction free energy for an ion of species i now reads

$$F_i(r) = z_i e_0 \psi(r) = \frac{z_i z^* e_0^2}{4\pi\epsilon_0\epsilon r} e^{-\frac{r}{l_D}} \ . \tag{44}$$

Similar precautions have to be taken when computing other quantities, such as the charge density.

Notably, the valence of an ion enters quadratically in the ionic strength, meaning that equivalent concentrations of ions with different valence result in a different value of I, thus affecting the electrostatic interactions in the solution. As a simple example, if we consider a solution of water with 150 mM of NaCl added, upon dissolution we end up with the two ions Na^+ and Cl^-, both with concentration 150 mM. The ionic strength is thus $I = (150\cdot(1)^2 + 150\cdot(-1)^2)$ mM $/2 = 150$ mM (since we were using the unit mM from the start rather than the number density, there is no need to divide by N_A), which corresponds to a Debye length equatl to $l_D \simeq 0.79$ nm. Now, let us consider a solution of water with 75 mM of $CaCl_2$ added. Upon dissolution, we end up with 75 mM of Ca^{2+} and 150 mM of Cl^-. The charge density is exactly the same as in the case above, however the ionic strength is now $I = (75 \cdot (2)^2 + 150 \cdot (-1)^2)$ mM $/2 = 225$ mM. The corresponding Debye length is $l_D \simeq 0.64$ nm, i.e. simply by changing the valency we have found a Debye length which is 23% smaller than in the monovalent case! In spite of this, as we show in Fig.3, the effect on the repulsion between similar ions is modest (blue continuous line and orange dashed line). In contrast, the prefactor $z^* z_i$ in the interaction energy boosts the repulsion for high-valency ions, as shown in the dotted green curve. Notably, the interaction energy in this case is larger than $k_B T$ even for $r = l_D$, indicating that the Debye-Hückel approximation does not hold well for this system.

As this example shows, higher valency results in general in stronger screening. Nevertheless, it has also to be noted that a lot of effects take place at moderate concentration when $z_i > 1$. Particularly, the electrostatic interaction has stronger effects than predicted by the Poisson-Boltzmann equation, which is a mean-field theory neglecting the presence of correlations between different ions.

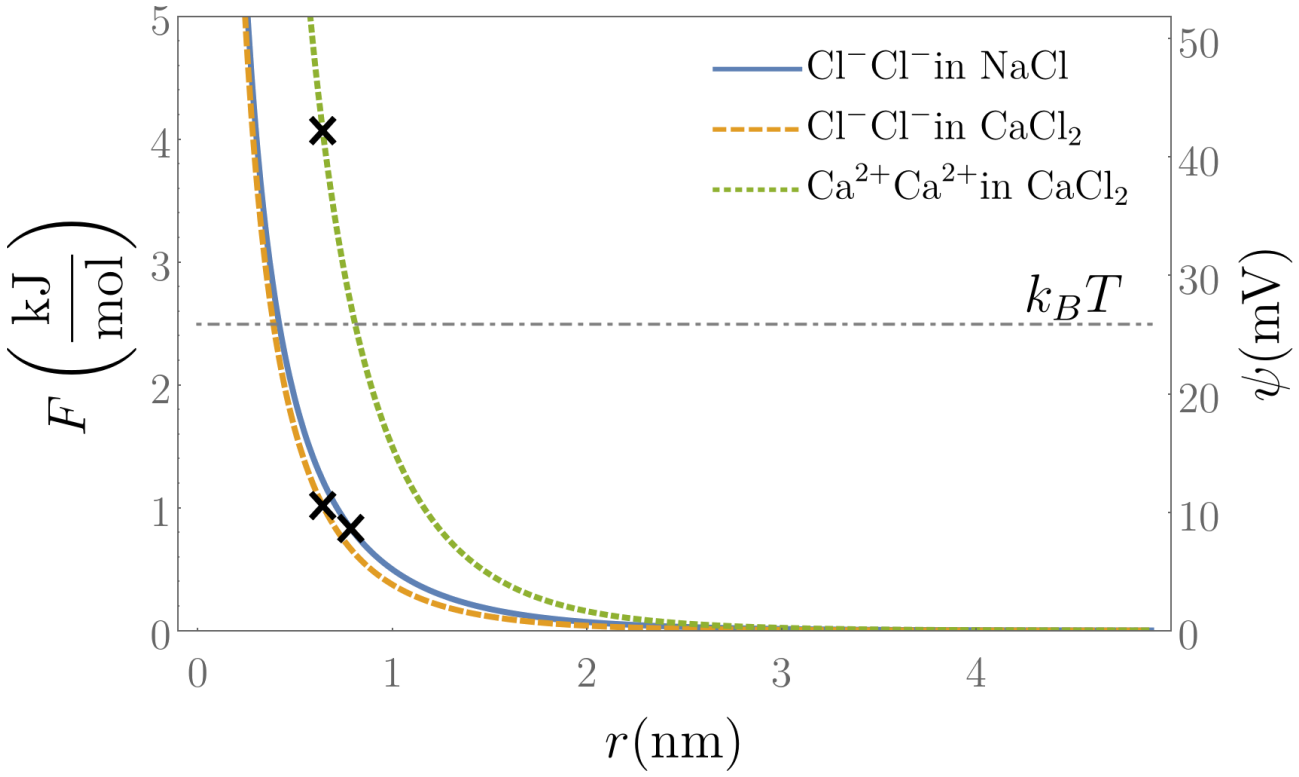

Figure 3: Debye-Hückel repulsive energy (left axis, Eq.(15)) and corresponding potential (right axis, Eq.(14)) as a function of distance for a solution containing 150 mM of NaCl and a second solution containing 75 mM of $CaCl_2$. In spite of having the same charge density, the two systems have different ionic strength, being equal to $I = 150$ mM and $I = 225$ mM for NaCl and $CaCl_2$, respectively. The blue continuous line corresponds to the repulsion between chlorides in the NaCl solution; the orange dashed line shows how this repulsion changes in $CaCl_2$ in spite of having the same charge concentration. The green dotted line shows the repulsion between the calcium ions in the same solution. The markers correspond to the Debye lengths of the solutions. The horizontal line shows the thermal energy k_BT and its corresponding potential $\psi \simeq 26$ mV.

5 Potential generated by a planar surface

When it comes to extended objects, the Poisson-Boltzmann equation can become quite complicated, although there are some cases in which the computations can be carried out with relative ease. One of the few cases in which the Poisson-Boltzmann equation can be solved exactly corresponds to the potential generated by a planar surface with a certain charge density $-\sigma e_0$, which is assumed negative to fix the ideas. The surface identifies two half-spaces corresponding to $z > 0$ and $z < 0$, where the reference frame was chosen such that the plane $z = 0$ corresponds to the surface itself. The region of negative z will be assumed to correspond to a bulk conductor, where the electric field is zero, i.e. $d\psi/dz = 0$ in this region. In contrast, $z > 0$ corresponds to a dielectric (e.g. water) with a dielectric constant ϵ. As we will show, the potential is weaker than the "standard" Coulomb case. Quite intringuingly, it also shows qualitatively-different behavior depending on whether salt is present in the solution or not.

5.1 Surface only

As a first point, we derive the potential generated by the charged surface in the absence of free ions, i.e. the standard Coulomb case. In the case of a planar surface, the symmetry of the system imposes that the potential depends only on the distance z from the surface. In order to properly solve Poisson's equation, we first consider the charges to be localized in a thin layer of thickness w, localized in the interval $-w \leq z \leq 0$. If A is the total extension of the surface, the total charge is equal to $-\sigma e_0 A$. However, given the thickness w of the layer, the total charge can also be written as $-\rho_0 e_0 A w$, where ρ_0 is the volume density of the charges in the layer. Equating the two formulas, we get $\rho_0 = \sigma/w$. Poisson's equation can be solved by considering the three regions corresponding to the conductor c ($z < -w$), the charged layer l ($-w \leq z \leq 0$) and the dielectric d ($z > 0$). Note that the charged layer is assumed to lie within the dielectric. The equation is written as

$$\begin{cases} \dfrac{d^2\psi_c(z)}{dz^2} = 0 & \text{if } z < -w \ , \\ \dfrac{d^2\psi_l(z)}{dz^2} = -\dfrac{-\rho_0 e_0}{\epsilon\epsilon_0} = \dfrac{\sigma e_0}{w\epsilon\epsilon_0} & \text{if } -w \leq z < 0 \ , \\ \dfrac{d^2\psi_d(z)}{dz^2} = 0 & \text{if } z \geq 0 \ . \end{cases} \tag{45}$$

Poisson's equation can be solved straightforwardly in the three regions by direct integration, leading to

$$\begin{cases} \psi_c(z) = A_c z + B_c & \text{if } z < -w \ , \\ \psi_l(z) = \dfrac{\sigma e_0}{2w\epsilon\epsilon_0} z^2 + A_l z + B_l & \text{if } -w \leq z < 0 \ , \\ \psi_d(z) = A_d z + B_d & \text{if } z \geq 0 \ , \end{cases} \tag{46}$$

where $A_c, B_c, A_l, B_l, A_d, B_d$ are constants to be determined. As we will see, the potential diverges for large z, thus preventing the possibility of using the usual boundary condition $\psi(\infty) = 0$. In the present case, we will instead set the zero of the potential for $z = 0$, i.e. $\psi(0) = 0$. The second boundary condition to be considered is the vanishing electric field in the conductor, i.e. $d\psi/dz = 0$ for $z \leq -w$. Finally, we will also impose the continuity of both the potential and the electric field at the interfaces[2]. To summarize, the boundary conditions are thus the following:

$$\begin{cases} \psi_d(0) = 0 \ , \\ \dfrac{d\psi_c}{dz}(z) = 0 \text{ for } z \leq -w \ , \\ \psi_c(-w) = \psi_l(-w) \ , \\ \dfrac{d\psi_c}{dz}(-w) = \dfrac{d\psi_l}{dz}(-w) \ , \\ \psi_l(0) = \psi_d(0) \ , \\ \dfrac{d\psi_l}{dz}(0) = \dfrac{d\psi_d}{dz}(0) \ . \end{cases} \tag{47}$$

Note that in order to determine the constants the condition $d\psi_c/dz(z) = 0$ for $z \leq -w$ can be substituted by $d\psi_c/dz(-w) = 0$. Substituting the formulas from Eq.(46), we obtain

$$\begin{cases} B_d = 0 \ , \\ A_c = 0 \ , \\ -A_c w + B_c = \dfrac{\sigma e_0}{2\epsilon\epsilon_0} w - A_l w + B_l \ , \\ A_c = -\dfrac{\sigma e_0}{\epsilon\epsilon_0} + A_l \ , \\ B_l = B_d \ , \\ A_l = A_d \ . \end{cases} \Rightarrow \begin{cases} A_c = 0 \ , \\ B_c = -\dfrac{\sigma e_0}{2\epsilon\epsilon_0} w \ , \\ A_l = \dfrac{\sigma e_0}{\epsilon\epsilon_0} \ , \\ B_l = 0 \ , \\ A_d = \dfrac{\sigma e_0}{\epsilon\epsilon_0} \ , \\ B_d = 0 \ . \end{cases} \tag{48}$$

The potential can thus be summarized as

$$\psi(z) = \begin{cases} -\dfrac{\sigma e_0}{2\epsilon\epsilon_0} w & \text{if } z \leq -w \ , \\ \dfrac{\sigma e_0}{2w\epsilon\epsilon_0} z^2 + \dfrac{\sigma e_0}{\epsilon\epsilon_0} z & \text{if } -w \leq z < 0 \ , \\ \boxed{\dfrac{\sigma e_0}{\epsilon\epsilon_0} z} & \text{if } z \geq 0 \ . \end{cases} \tag{49}$$

[2]Note that in many textbooks it is shown that the electric field is discontinuous at a charged surface. This is of course correct, but it is avoided here by introducing the finite thickness w of the charged object. Taking the limit $w \to 0$ and comparing the regions $z > 0$ and $z < 0$ results in the discontinuity usually seen in textbooks.

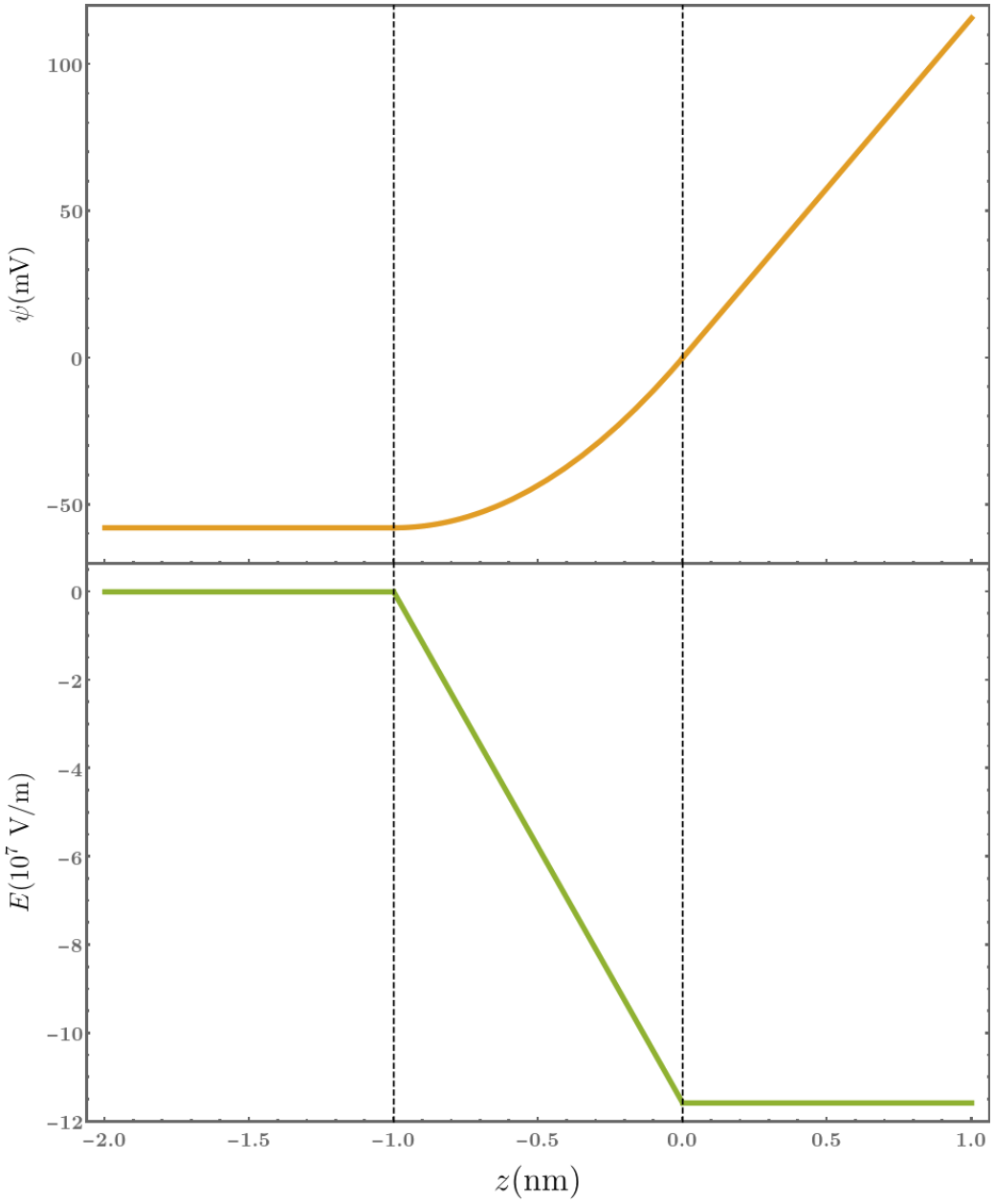

Figure 4: Potential (top) and electric field (bottom) generated by a negatively-charged slab with density $\sigma = 0.5$ nm^{-2} and thickness $w = 1$ nm.

The corresponding electric field can be easily computed as $E = -d\psi/dz$, giving

$$E(z) = \begin{cases} 0 & \text{if } z \leq -w \ , \\ -\dfrac{\sigma e_0}{w\epsilon\epsilon_0} z - \dfrac{\sigma e_0}{\epsilon\epsilon_0} & \text{if } -w \leq z < 0 \ , \\ -\dfrac{\sigma e_0}{\epsilon\epsilon_0} & \text{if } z \geq 0 \ . \end{cases} \tag{50}$$

$\psi(z)$ and $E(z)$ are reported in Fig.4 for a surface with $\sigma = 0.5$ nm^{-2} and $w = 1$ nm. As mentioned above, the potential diverges linearly for $|z| \to \infty$, which corresponds to a constant electric field. Note that E is the measurable quantity (that is, the corresponding force exerted on a charge placed at a certain position), so that the divergence of ψ is not a problem as long as E is finite. It is also worth noting that the magnitude of the electric field is different than the value $\sigma e_0/(2\epsilon\epsilon_0)$ usually found in textbooks by a factor of 2. This difference arises from the fact that here we assumed that $z < 0$ corresponds to a conductor ($d\psi/dz = 0$), while the problem considered in textbooks usually studies a system where there is dielectric on both sides. Here, we opted for this system because it enables a more direct comparison with the cases with mobile charges.

5.2 Counterions only

We now consider the case in which a surface is put in an overall electroneutral solution with free ions. We assume that only counterions are present in a suitable amount to compensate for the charge density of the surface, which is assumed to be constant. Let A be the extension of the surface, then the total negative charge is $Q_- = -\sigma e_0 A$. If $\rho_+(z)$ is the concentration of counterions, then the total positive charge $Q_+ = \int_0^\infty \rho_+(z) e_0 \cdot A dz = A e_0 \int_0^\infty \rho_+(z) dz$. Electroneutrality thus implies

$$Q_+ + Q_- = 0 \Rightarrow \sigma = \int_0^\infty \rho_+(z) dz \ . \tag{51}$$

To determine the potential generated by the surface in the presence of only counterions, we resort again to the Poisson-Boltzmann equation. Note that, differently than in the case of the Debye-Hückel potential studied above, here only one exponential term is present, since there are only counterions in the solution. Indicating as $\rho_{0,+}$ the density of counterions at the surface (where we set[3] $\psi(0) = 0$), the Boltzmann distribution gives that $\rho_+(z) = \rho_{0,+} e^{-e_0\psi(z)/(k_B T)}$, where the minus sign in the exponential stems from our choice of positive counterions. The Poisson-Boltzmann equation thus reads

$$\frac{d^2\psi}{dz^2} = -\frac{e_0\rho_+}{\epsilon_0\epsilon} = -\frac{e_0\rho_{0,+}}{\epsilon_0\epsilon}\, e^{-\frac{e_0\psi(z)}{k_B T}} \quad \text{if } z > 0 \ , \tag{52}$$

As for the boundary conditions, we set one of them by assigning $\psi(0) = 0$, as mentioned above. The second condition can be obtained by noting that for $z \to \infty$ we expect $d\psi/dz \to 0$, based on the observation that the weakening of the electrostatic interaction with respect to the pure Coulombic case (where $d\psi/dz$ is constant) leads to a vanishing field at large distance. As for the potential itself, we expect that it increases as a function of z, since the surface is charged negatively and the minimum potential is thus expected to be attained at $z = 0$. There

[3] In this case, we cannot set the zero of the potential at infinity, since the potential diverges at large distances, as explained below.

are two possibilities when $z \to \infty$: either ψ diverges, or it converges to a finite value ψ_∞. Assuming the latter case, this would mean that the counterion density reaches a plateau value equal to $\rho_{0,+}e^{-e_0\psi_\infty/(k_BT)} > 0$. Therefore, the integral $\int_0^\infty \rho_+ dz = \int_0^\infty \rho_{0,+}e^{-e_0\psi/(k_BT)}dz$ would diverge, which is in contrast with the electroneutrality condition, Eq.(51). Based on these considerations, we can thus conclude that $\psi \to \infty$ for large z. The divergence of the potential, in analogy with the case of the Coulombic potential generated by a "bare" surface, prevents the employment of the Debye-Hückel approximation to linearize the Poisson-Boltzmann equation, since a low potential can be found only in close proximity of $z = 0$, where we assume $\psi(0) = 0$; luckily, in this case the full nonlinear equation can be solved analytically. To summarize, the Poisson-Boltzmann equation and its boundary conditions thus read

$$\begin{cases} \dfrac{d^2\psi}{dz^2} = -\dfrac{e_0\rho_-}{\epsilon_0\epsilon} = -\dfrac{e_0\rho_{0,+}}{\epsilon_0\epsilon}\, e^{-\frac{e_0\psi(z)}{k_BT}} \quad \text{if } z > 0\ , \\ \psi(0) = 0\ , \\ \dfrac{d\psi}{dz}(\infty) = 0\,, \psi(\infty) = +\infty\ . \end{cases} \tag{53}$$

In order to solve this differential equation, we define the adimensionalized potential $u \equiv e_0\psi/(k_BT) \Rightarrow \psi = (k_BT/e_0)u \Rightarrow d\psi/dz = (k_BT/e_0)du/dz \Rightarrow d^2\psi/dz^2 = (k_BT/e_0)d^2u/dz^2$. Hence, the equation becomes

$$\begin{cases} \dfrac{k_BT}{e_0}\dfrac{d^2u}{dz^2} = -\dfrac{e_0\rho_{0,+}}{\epsilon_0\epsilon}\, e^{-u} \Rightarrow \dfrac{d^2u}{dz^2} = -\dfrac{e_0^2\rho_{0,+}}{\epsilon_0\epsilon k_BT}\, e^{-u} = -4\pi l_B\rho_{0,+}\, e^{-u}\ , \\ u(0) = 0\ , \\ \dfrac{du}{dz}(\infty) = 0\,, u(\infty) = +\infty\ , \end{cases} \tag{54}$$

where we used the definition of the Bjerrum length, $l_B = e_0^2/(4\pi k_BT\epsilon_0\epsilon)$. The differential equation can be solved by multiplying both sides by du/dz, obtaining

$$\frac{du}{dz}\frac{d^2u}{dz^2} = -4\pi l_B\rho_{0,+}\frac{du}{dz}\, e^{-u}\ . \tag{55}$$

Now, we note that

$$\begin{cases} \dfrac{du}{dz}\dfrac{d^2u}{dz^2} = \dfrac{1}{2}\dfrac{d}{dz}\left(\dfrac{du}{dz}\right)^2\ , \\ \dfrac{du}{dz}\, e^{-u} = -\dfrac{d}{dz}e^{-u}\ . \end{cases} \tag{56}$$

Therefore, the Poisson-Boltzmann equation can be written as

$$\frac{d}{dz}\left[\frac{1}{2}\left(\frac{du}{dz}\right)^2\right] = 4\pi l_B\rho_{0,+}\frac{d}{dz}\, e^{-u}\ . \tag{57}$$

Integrating both sides, we thus obtain

$$\left(\frac{du}{dz}\right)^2 = 8\pi l_B \rho_{0,+}\, e^{-u} + C\ , \tag{58}$$

where C is an integration constant to be determined. To this aim, we employ the second boundary condition ($du/dz(\infty) = 0, u(\infty) = +\infty$), from which we conclude that $C = 0$. Substituting the constant in Eq.(58) and taking the square root, we thus obtain

$$\frac{du}{dz} = \sqrt{8\pi l_B \rho_{0,+}\, e^{-u}} = \sqrt{8\pi l_B \rho_{0,+}} e^{-\frac{u}{2}}\ , \tag{59}$$

where we considered the positive solution since ψ (and thus u) is an increasing function of z, due to the negative sign of the charges present on the surface. Rearranging, separating the variables and integrating, we thus obtain

$$\begin{aligned}
&\int_{u(0)=0}^{u} e^{\frac{u'}{2}} du' = \sqrt{8\pi l_B \rho_{0,+}} \int_0^z dz' \Rightarrow \\
&2\left(e^{\frac{u}{2}} - 1\right) = \sqrt{8\pi l_B \rho_{0,+}} \cdot z \Rightarrow \\
&e^{\frac{u}{2}} = 1 + \sqrt{2\pi l_B \rho_{0,+}} \cdot z \equiv 1 + \frac{z}{l_{GC}} \Rightarrow \\
&u = 2\ln\left(1 + \frac{z}{l_{GC}}\right) \Rightarrow \\
&\boxed{\psi(z) = \frac{2k_B T}{e_0} \ln\left(1 + \frac{z}{l_{GC}}\right)}\ ,
\end{aligned} \tag{60}$$

where l_{GC} is a constant known as *Gouy-Chapman length* and defined as

$$l_{GC} \equiv \frac{1}{\sqrt{2\pi l_B \rho_{0,+}}}\ . \tag{61}$$

Note that the boundary condition $u(0) = 0$ has been used in the first step of Eq.(60).

Eq.(60) depends on the counterion density $\rho_{0,+}$ in the proximity of the surface via the Gouy-Chapman length l_{GC}. It is expected that $\rho_{0,+}$ is determined by the surface charge density σ; the explicit dependence can be obtained straightforwardly from electroneutrality. Making use of the Poisson-Boltzmann equation, Eq.(51) can be written as

$$\sigma = \int_0^\infty \rho_+(z) dz = -\frac{\epsilon_0 \epsilon}{e_0} \int_0^\infty \frac{d^2\psi}{dz^2} dz = -\frac{\epsilon_0 \epsilon}{e_0} \left.\frac{d\psi}{dz}\right|_0^\infty = \frac{\epsilon_0 \epsilon}{e_0} \frac{d\psi}{dz}(0) \Rightarrow \frac{d\psi}{dz}(0) = \frac{e_0 \sigma}{\epsilon_0 \epsilon}\ , \tag{62}$$

where we made use of the boundary condition $d\psi/dz(\infty) = 0$. Note that this is equivalent to assume that the electric field at the surface is the same as in the Coulomb case, which is

similar in spirit to our derivation of the Debye-Hückel formula for the case of small ions. The combination of Eq.(62) and Eq.(60) enables writing l_{GC} as a function of the surface density σ.

$$\frac{d\psi}{dz}(0) = \frac{e_0\sigma}{\epsilon_0\epsilon} \Rightarrow \frac{2k_BT}{e_0\, l_{GC}} = \frac{e_0\sigma}{\epsilon_0\epsilon} \Rightarrow \boxed{l_{GC} = \frac{2k_BT\epsilon_0\epsilon}{e_0^2\sigma} = \frac{1}{2\pi l_B\sigma}}\,. \tag{63}$$

Comparing with the definition of l_{GC} given above also shows that the counterion density at the surface is $\rho_{0,+} = 2\pi l_B\sigma^2$.

From Eq.(60) we see that the potential still diverges for large z, coherently with our considerations above. However, the screening effect of counterions makes ψ weaker than in the Coulombic case, showing only a logarithmic increase with z compared to the linear increase obtained in the case of a bare surface. The potential is plotted in Fig.5a as a green dashed line together with the result obtained in the case of a bare surface (yellow continuous curve, Eq.(49)) and the one found in the presence of salt (red dotted line, see next section). The plot clearly indicates the weakening effect of the counterions on the potential.

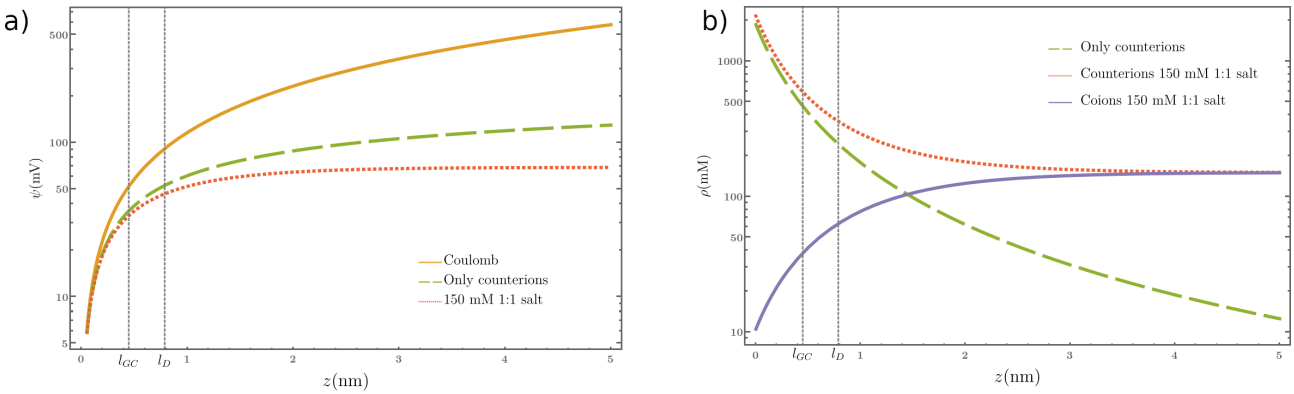

Figure 5: a) Potential generated by a negatively-charged surface with density $\sigma = 0.5$ nm^{-2} without mobile ions (yellow continuous line), with only counterions (green dashed line) and in the presence of 150 mM of monovalent salt (red dotted line). Vertical lines indicate the Gouy-Chapman length l_{GC} corresponding to the chosen σ and the Debye length l_D corresponding to the chosen ionic strength. b) Distance-dependent concentrations of counterions in the absence of salt (green dashed line), and of counterions and coions in the presence of 150 mM of salt (red dotted line and purple continuous line, respectively).

5.2.1 Counterions distribution

The counterions distribution is found as

$$\rho_+(z) = -\frac{\epsilon_0\epsilon}{e_0}\frac{d^2\psi}{dz^2} = -\frac{\epsilon_0\epsilon}{e_0}\cdot\left[-\frac{2k_BT}{e_0}\frac{1}{(l_{GC}+z)^2}\right] = \frac{1}{2\pi l_B}\frac{1}{(l_{GC}+z)^2} = \frac{l_{GC}\,\sigma}{(l_{GC}+z)^2}\,, \tag{64}$$

that is

$$\boxed{\rho_+(z) = \frac{l_{GC}\,\sigma}{(l_{GC}+z)^2}}\,. \tag{65}$$

Therefore, the counterions distribution decays algebraically from its maximum value ($\rho_+(0) = \sigma/l_{GC}$), as shown in Fig.5b (green dashed line).

It is interesting to compute the fraction $\varphi(z)$ of counterions contained within a distance z, which is easily computed by integrating Eq.(65). Since electroneutrality imposes that $\int_0^\infty \rho_+(z)dz = \sigma$, $\varphi(z)$ is obtained as

$$\varphi(z) = \frac{1}{\sigma}\int_0^z \rho_+(z')dz' = \frac{1}{\sigma}\int_0^z \frac{l_{GC}\,\sigma}{(l_{GC}+z')^2}dz' = l_{GC}\cdot\left(-\frac{1}{l_{GC}+z'}\right)\Bigg|_{z'=0}^{z} = \frac{z}{l_{GC}+z}\,. \tag{66}$$

Substituting $z = l_{GC}$ gives $\varphi(l_{GC}) = 0.5$, i.e. half the counterions are contained within a layer of thickness l_{GC}, which serves to give a physical interpretation of the Gouy-Chapman length as setting the length scale within which most of the counterions are found.

5.2.2 Scaling argument

The results obtained in the previous section can be rationalized by some simple scaling arguments. As usual, we do not consider numerical prefactors in this kind of considerations. The scaling argument is based in comparing the electrostatic energy of a counterion and its entropy, which is estimated by considering an ideal gas. The electrostatic energy of a counterion can be obtained as $U_e = \psi \cdot e_0$, where ψ is the potential generated by the bare surface. From Eq.(49), we thus estimate $\psi \sim \sigma e_0 z/(\epsilon_0\epsilon)$, so that the electrostatic energy is $U_e \sim \sigma e_0^2 z/(\epsilon_0\epsilon) \sim \sigma \cdot k_B T l_B \cdot z \sim k_B T z/l_{GC}$. As for the entropy, one has $TS \sim k_B T \ln V$, where V is the volume of the region considered. In the present system, $V \sim A \cdot z$, where A is the (constant) extension of the surface, so that by dropping the term independent of z we obtain $TS \sim k_B T \ln z$. Since U_e increases linearly with distance and TS only logarithmically, it is expected that the energy dominates at large length scales, while at small length scales it is overcomed by entropy. The threshold between these two regimes is found when[4] $U_e \sim k_B T \Rightarrow z \sim l_{GC}$. Therefore, this scaling argument depicts the system as a cloud of counterions contained within a layer of thickness l_{GC} in proximity of the surface, which is in good agreement with the results obtained above.

5.3 With salt

The presence of added salt in solution changes drastically the physical picture. First of all, we note that at large distances the concentration of counterions and coions is expected to take

[4]In scaling arguments, the logarithmic term is usually dropped when compared to a power law, since for large enough scales they differ by orders of magnitude.

a *finite* value, corresponding to the bulk concentration of salt ρ_∞. Hence, at difference with the case with only counterions, the difference $\psi(\infty) - \psi(0)$ is finite, i.e. the potential does not diverge. A second key difference is that the Poisson-Boltzmann equation now has two source terms, corresponding to positive and negative charges, exactly in the same way as for the Debye-Hückel potential. Given the lack of divergence of the potential, and since it simplifies the calculations, we fix the zero of the potential at infinite, i.e. $\psi(\infty) = 0$. This enables writing the Poisson-Boltzmann equation directly in terms of the bulk concentration of salt

$$\frac{d^2\psi}{dz^2} = -\frac{e_0\rho_\infty}{\epsilon_0\epsilon}\left(e^{-\frac{e_0\psi}{k_BT}} - e^{\frac{e_0\psi}{k_BT}}\right) = \frac{2e_0\rho_\infty}{\epsilon_0\epsilon}\sinh\frac{e_0\psi}{k_BT} \ . \tag{67}$$

Note that the contribution of the counterions balancing the surface charge (i.e. not coming from the salt) is also included in the previous equation, since the corresponding bulk concentration is zero. Electroneutrality can be written in the same terms as before:

$$\sigma = \int_0^\infty (\rho_+ - \rho_-)dz = -\frac{\epsilon_0\epsilon}{e_0}\int_0^\infty \frac{d^2\psi}{dz^2}dz = -\frac{\epsilon_0\epsilon}{e_0}\left.\frac{d\psi}{dz}\right|_0^\infty = \frac{\epsilon_0\epsilon}{e_0}\frac{d\psi}{dz}(0) \Rightarrow \frac{d\psi}{dz}(0) = \frac{e_0\sigma}{\epsilon_0\epsilon} \ . \tag{68}$$

The complete problem including differential equations and boundary conditions is thus

$$\begin{cases} \dfrac{d^2\psi}{dz^2} = \dfrac{2e_0\rho_\infty}{\epsilon_0\epsilon}\sinh\dfrac{e_0\psi}{k_BT} \quad \text{if } z > 0 \ , \\ \psi(\infty) = 0 \ , \\ \dfrac{d\psi}{dz}(0) = \dfrac{e_0\sigma}{\epsilon_0\epsilon} \ . \end{cases} \tag{69}$$

Note that in this case it makes sense to consider the Debye-Hückel approximation for low potential, since ψ is always finite. Nevertheless, we can do better than this: we will solve the full nonlinear equation. As in the previous section, we define the adimensionalized potential $u \equiv e_0\psi/(k_BT) \Rightarrow \psi = (k_BT/e_0)u \Rightarrow d\psi/dz = (k_BT/e_0)du/dz \Rightarrow d^2\psi/dz^2 = (k_BT/e_0)d^2u/dz^2$. Hence, the equation becomes

$$\begin{cases} \dfrac{k_BT}{e_0}\dfrac{d^2u}{dz^2} = \dfrac{2e_0\rho_\infty}{\epsilon_0\epsilon}\sinh u \Rightarrow \dfrac{d^2u}{dz^2} = \dfrac{2e_0^2\rho_\infty}{\epsilon_0\epsilon k_BT}\ \sinh u = 8\pi l_B\rho_\infty\ \sinh u = \dfrac{\sinh u}{l_D^2} \ , \\ u(\infty) = 0 \ , \\ \dfrac{k_BT}{e_0}\dfrac{du}{dz}(0) = \dfrac{e_0\sigma}{\epsilon_0\epsilon} \Rightarrow \dfrac{du}{dz}(0) = \dfrac{e_0^2\sigma}{\epsilon_0\epsilon k_BT} = 4\pi l_B\sigma \ , \end{cases} \tag{70}$$

where we used the defintions of the Bjerrum length, $l_B = e_0^2/(4\pi k_BT\epsilon_0\epsilon)$, and of the Debye length, $l_D = 1/\sqrt{8\pi l_B\rho_\infty}$. Proceeding as before, we multiply both sides by du/dz, obtaining

$$\frac{du}{dz}\frac{d^2u}{dz^2} = \frac{1}{l_D^2}\frac{du}{dz}\ \sinh u \ . \tag{71}$$

Now, we note that

$$\begin{cases} \dfrac{du}{dz}\dfrac{d^2u}{dz^2} = \dfrac{1}{2}\dfrac{d}{dz}\left(\dfrac{du}{dz}\right)^2 , \\ \dfrac{du}{dz}\ \sinh u = \dfrac{d}{dz}\cosh u\ . \end{cases} \tag{72}$$

Therefore, the Poisson-Boltzmann equation can be written as

$$\frac{d}{dz}\left[\frac{1}{2}\left(\frac{du}{dz}\right)^2\right] = \frac{1}{l_D^2}\frac{d}{dz}\ \cosh u\ . \tag{73}$$

Integrating both sides, we thus obtain

$$\left(\frac{du}{dz}\right)^2 = \frac{2}{l_D^2}\ \cosh u + C\ , \tag{74}$$

where C is an integration constant to be determined. Using the boundary condition $u(\infty) = 0$ and observing that $du/dz \to 0$, for large z, we conclude that $C = -2/l_D^2$. Hence

$$\left(\frac{du}{dz}\right)^2 = \frac{2}{l_D^2}\ (\cosh u - 1)\ , \tag{75}$$

Making use of the formula $\cosh u - 1 = 2\sinh^2(u/2)$, we can write

$$\left(\frac{du}{dz}\right)^2 = \frac{4}{l_D^2}\ \sinh^2\frac{u}{2} \Rightarrow \frac{du}{dz} = -\frac{2}{l_D}\sinh\frac{u}{2} = \frac{2}{l_D}\sinh\left(-\frac{u}{2}\right)\ . \tag{76}$$

In the previous formula, we have considered the minus sign because u is an increasing function of z, i.e. $du/dz > 0$, and took into account that the positive derivative together with the condition $u(\infty) = 0$ implies that $u < 0$. Separating the variables, integrating and making use of the formula $\int du/\sinh(-u/2) = -2\ln\tanh(-u/4)$, we find

$$-2\ln\tanh\left(-\frac{u}{4}\right) = \frac{2z}{l_D} - 2\ln(-\gamma) \Rightarrow \ln\tanh\left(-\frac{u}{4}\right) = -\frac{z}{l_D} + \ln(-\gamma)\ , \tag{77}$$

where $\gamma < 0$ is the integration constant, which was written by means of a logarithm for mathematical convenience. Substituting $z = 0$, we see that $\gamma = \tanh[e_0\psi(0)/(4k_BT)] < 0$. In order to determine its value, we consider the remaining boundary condition (electroneutrality). We note that

$$\frac{d}{dz}\ln\tanh\left(-\frac{u}{4}\right) = \frac{1-\tanh^2\left(-\frac{u}{4}\right)}{\tanh\left(-\frac{u}{4}\right)}\cdot\left(-\frac{1}{4}\right)\cdot\frac{du}{dz}\ , \tag{78}$$

which for $z = 0$ gives (remember that the boundary condition gives $du/dz(0) = 4\pi l_B\sigma = 2/l_{GC}$)

$$\frac{d}{dz}\ln\tanh\left(-\frac{u}{4}\right)(z=0) = \frac{1-\gamma^2}{-\gamma}\cdot\left(-\frac{1}{4}\right)\cdot\frac{2}{l_{GC}} = \frac{1-\gamma^2}{2\gamma\, l_{GC}}\ . \tag{79}$$

From Eq.(77), we also obtain that

$$\frac{d}{dz}\ln\tanh\left(-\frac{u}{4}\right)(z=0) = -\frac{1}{l_D}\,, \tag{80}$$

so that γ is determined in the following way:

$$\frac{1-\gamma^2}{2\gamma\, l_{GC}} = -\frac{1}{l_D} \Rightarrow \gamma^2 - 2\frac{l_{GC}}{l_D}\gamma - 1 = 0 \Rightarrow \boxed{\gamma = \frac{l_{GC}}{l_D} - \sqrt{\left(\frac{l_{GC}}{l_D}\right)^2 + 1}} \tag{81}$$

where we retained only the physically-meaning solution yielding $\gamma < 0$. Proceeding in the computation of the potential, we find from Eq.(77)

$$u = -4\,\mathrm{atanh}\left(-\gamma e^{-\frac{z}{l_D}}\right) \Rightarrow \psi = -\frac{4k_BT}{e_0}\,\mathrm{atanh}\left(-\gamma e^{-\frac{z}{l_D}}\right)\,. \tag{82}$$

Making use of the formula $\mathrm{atanh}\, x = (1/2)\ln[(1+x)/(1-x)]$, we obtain

$$\boxed{\psi(z) = -\frac{2k_BT}{e_0}\ln\frac{1-\gamma e^{-\frac{z}{l_D}}}{1+\gamma e^{-\frac{z}{l_D}}}}\,, \tag{83}$$

which is the *Gouy-Chapman formula* for the potential generated by a surface in the presence of salt. This potential is weaker than both the one generated by a bare surface, Eq.(49), and the one obtained when only counterions are present, Eq.(60). This is evidenced in Fig.5a, where the potential from Eq.(83) for a solution containing 150 mM of monovalent salt (red dotted line) is plotted alongside the other two cases obtained for the same σ. In order to enable a proper comparison, in the plot we have shifted the zero of the potential in the case of salt, setting $\psi(0) = 0$. In other words, considering Eq.(83) we have actually plotted $\psi(z) + (2k_BT/e_0)\ln[(1-\gamma)/(1+\gamma)]$.

Problem. Show that in the Debye-Hückel approximation the potential is $\psi(z) \simeq \psi_0\, e^{-z/l_D}$. It is best if you try two alternative routes, namely by applying the Debye-Hückel approximation in the original Poisson-Boltzmann equation, Eq.(69), or by considering a weak potential in the final result, Eq.(83).

5.3.1 Grahame equation

As a further note, we stress that there is a direct relation between the surface density σ, the bulk salt concentration ρ_∞ and the surface potential $\psi(0) \equiv \psi_0$. Indeed, rearranging Eq.(81),

and remembering that $l_{GC} = 1/(2\pi l_B \sigma)$ and $l_D = 1/\sqrt{8\pi l_B \rho_\infty}$, we can write

$$\begin{aligned}
&\frac{1-\gamma^2}{2\gamma\, l_{GC}} = -\frac{1}{l_D} \Rightarrow \\
&\pi l_B \sigma \frac{1-\gamma^2}{\gamma} = -\sqrt{8\pi l_B \rho_\infty} \Rightarrow \\
&\sigma = -\sqrt{\frac{8\rho_\infty}{\pi l_B}} \frac{\gamma}{1-\gamma^2} = \\
&-\sqrt{\frac{8\rho_\infty}{\pi l_B}} \frac{\tanh \frac{e_0\psi_0}{4k_BT}}{1-\tanh^2 \frac{e_0\psi_0}{4k_BT}} = \\
&-\sqrt{\frac{8\rho_\infty}{\pi l_B}} \tanh \frac{e_0\psi_0}{4k_BT} \cosh^2 \frac{e_0\psi_0}{4k_BT} = \\
&-\sqrt{\frac{8\rho_\infty}{\pi l_B}} \sinh \frac{e_0\psi_0}{4k_BT} \cosh \frac{e_0\psi_0}{4k_BT} = \\
&-\sqrt{\frac{2\rho_\infty}{\pi l_B}} \sinh \frac{e_0\psi_0}{2k_BT} \,,
\end{aligned} \tag{84}$$

where we made use of the formulas $1 - \tanh^2 x = 1/\cosh^2 x$ and $\sinh 2x = 2 \sinh x \cosh x$. The final formula

$$\boxed{\sigma = \sqrt{\frac{2\rho_\infty}{\pi l_B}} \sinh\left(-\frac{e_0\psi_0}{2k_BT}\right)} \tag{85}$$

is the relationship sought between σ, ρ_∞ and ψ_0, and is known as *Grahame equation*. This formula comes in hand e.g. to determine σ from measurements of ψ_0 at controlled values of salt. Making use of the formula $\sinh 2x = 2\tanh x/(1-\tanh^2 x)$ and remembering that $\gamma = \tanh(e\psi_0/(4k_BT))$, the Grahame equation can also be written as

$$\sigma = -\sqrt{\frac{8\rho_\infty}{\pi l_B}} \frac{\gamma}{1-\gamma^2} \,. \tag{86}$$

Remember that, due to our choice of a negatively-charged surface and $\psi(\infty) = 0$, the potential is negative everywhere, hence $-1 \leq \gamma \leq 0$.

It is also worth noting that in the Debye-Hückel approximation, $e_0\psi/(k_BT) \ll 1$, one obtains (remember that $\sinh x \simeq x$ for $x \ll 1$ and that $l_B = e_0^2/(4\pi k_B T \epsilon_0 \epsilon)$)

$$\sigma \simeq \sqrt{\frac{2\rho_\infty}{\pi l_B}} \cdot \left(-\frac{e_0\psi_0}{2k_BT}\right) = -\sqrt{\frac{2\rho_\infty}{\pi l_B}} \cdot \frac{e_0\psi_0}{2k_BT} \cdot \frac{l_B}{\frac{e_0^2}{4\pi k_B T \epsilon_0 \epsilon}} = -\sqrt{8\pi\rho_\infty l_B} \cdot \frac{\epsilon_0\epsilon}{e_0} \cdot \psi_0 \,. \tag{87}$$

Since by definition $l_D = 1/\sqrt{8\pi\rho_\infty l_B}$, we thus obtain

$$\psi_0 \simeq -\frac{\sigma e_0}{\epsilon_0 \epsilon} l_D \ , \tag{88}$$

which is the potential difference generated by a capacitor of surface density σ and thickness l_D. Therefore, within the Debye-Hückel approximation the system in the vicinity of the surface behaves as if one had two layers of charge density $\pm e_0\sigma$ at distance l_D, which originated the name *(diffusive) electric double layer* for this kind of systems.

5.3.2 Ion distributions

From the potential, the Boltzmann weight $e_0\psi/(k_BT)$ can be easily determined as

$$\frac{e_0\psi(z)}{k_BT} = -2\ln\frac{1-\gamma e^{-\frac{z}{l_D}}}{1+\gamma e^{-\frac{z}{l_D}}} \ . \tag{89}$$

The density of (positive) counterions is obtained as $\rho_+(z) = \rho_\infty e^{-e_0\psi/(k_BT)}$, i.e.

$$\boxed{\rho_+(z) = \rho_\infty \left(\frac{1-\gamma e^{-\frac{z}{l_D}}}{1+\gamma e^{-\frac{z}{l_D}}}\right)^2} \ . \tag{90}$$

Analogously, the density of (negative) coions is found as $\rho_-(z) = \rho_\infty e^{e_0\psi/(k_BT)}$, i.e.

$$\boxed{\rho_-(z) = \rho_\infty \left(\frac{1+\gamma e^{-\frac{z}{l_D}}}{1-\gamma e^{-\frac{z}{l_D}}}\right)^2} \ . \tag{91}$$

These two formulas are plotted in Fig.5b as a red dotted line (ρ_+) and a purple continuous line (ρ_-) for 150 mM of monovalent salt. Two key differences with respect to the case in which there is no salt (green dashed line, Eq.(65) can be outlined for the counterions. The first difference is in the length scale determining the decay, which in absence of salt is the Gouy-Chapman length l_{GC}, while in this case it is the Debye length l_D. The second difference is in the decay itself, which passes from being algebraic to exponential.

5.3.3 Charge regulation

In our previous derivation, we have assumed that the surface charge is constant, i.e. it is independent of the amount of salt added to the solution, ρ. In reality this is not actually the case, since there is an exchange of ions between the surface and the solution, so that in general some ions will be bound. In order to characterize this ion exchange, we consider the *dissociation constant* K_d. For two species A and B forming a complex AB, by definition

$$K_d = \frac{[A]\cdot[B]}{[AB]} \tag{92}$$

where $[\dots]$ indicates the equilibrium concentration of a species. In the present case, the species are the ionized groups S^- of the surface (assumed negative to fix the ideas) and the positive counterions X^+ that can bind on the groups. Note that these ions can be coming from the salt or not, as we will see below. Note that the binding takes place in the vicinity of the surface, so that if the bulk concentration of the binding counterions is $[X^+]_\infty$, the actual concentration to be considered is[5] $[X^+] = [X^+]_\infty e^{-e_0\psi_0/(k_BT)}$. As for the surface, by defining the fraction α of ionized groups, we have $[S^-] = \alpha\sigma/w$ and $[SX] = (1-\alpha\sigma)/w$, where w is the thickness of the layer corresponding to the groups (its value is irrelevant in this context because it will be canceled out). The dissociation constant can thus be written as

$$K_d = \frac{[S^-][X^+]}{[SX]} = \frac{\alpha\frac{\sigma}{w}}{(1-\alpha)\frac{\sigma}{w}} \cdot [X^+]_\infty e^{-\frac{e_0\psi_0}{k_BT}} = \frac{\alpha}{1-\alpha}[X^+]_\infty e^{-\frac{e_0\psi_0}{k_BT}} \ . \tag{93}$$

Note that in the previous equation there are two unknowns, namely ψ_0 and α. Rerranging, we can determine α:

$$\alpha = \frac{1}{1 + \frac{[X^+]_\infty}{K_d} e^{-\frac{e_0\psi_0}{k_BT}}} \ . \tag{94}$$

A second equation can be obtained by observing that Grahame's equation can still be applied

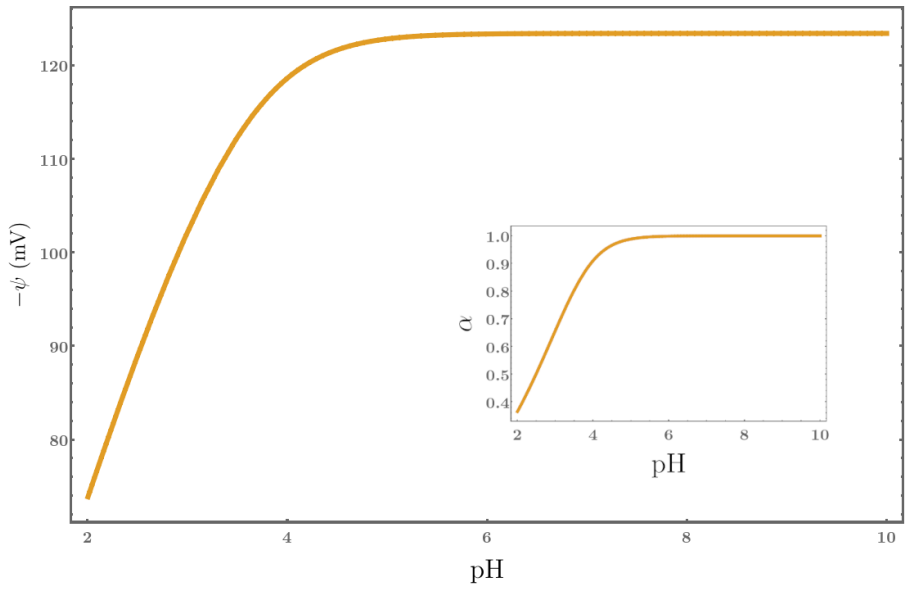

Figure 6: pH dependence of the potential generated by a surface whose negatively-charged groups can bind protons. Inset: Corresponding fraction α of ionized groups.

[5]The total concentration of counterions is actually equal to $[X^+] + [SX]$, but we assume that binding does not perturb the concentration of free ions.

to the effective surface density $\alpha\sigma$, i.e.

$$\alpha\sigma = \sqrt{\frac{2\rho_\infty}{\pi l_B}} \sinh\left(-\frac{e_0\psi_0}{2k_BT}\right) \tag{95}$$

In this way, both α and ψ_0 can be determined from knowledge of $[X^+]_\infty$, σ, ρ_∞ and K_d. Importantly, the solution depends on the amount of salt. Also, we will find a nontrivial solution (α significantly smaller than 1) only when $[X^+]_\infty$ is comparable to or smaller than K_d.

A particularly important case is provided by binding of protons H^+, since in this case the bulk concentration of the binding species will be determined directly by the pH of the solution as $[H^+]_\infty = 10^{-\mathrm{pH}}$. As an example, we report in Fig.6 the pH dependence of the potential generated by a surface where ionizable groups are present with a density $\sigma = 1.25$ nm^{-2} and where protons can bind with a dissociation constant $K_d = 0.1$ mM. The solution contains 100 mM of monovalent salt.

5.3.4 Example: charge density and potential generated by a lipid membrane

As an example of the usage of the Gouy-Chapman theory in the real world, we report the results of a study conducted on lipid membranes[6]. In this work, the authors considered membranes formed by mixtures of the lipid dioleoylphosphatidylserine (we will refer to it as PS from now on) and dioleoylphosphatidylcholine (PC). Under the conditions considered, PS was negatively charged, while PC was zwitterionic (i.e. with both positive and negative charges present), although for the present purposes we will consider it as neutral. Several mixtures were prepared with different relative amounts of the two lipids, characterized by the mole fraction X_{PS} of PS, and put in a solution containing a Tris buffer (a typical cocktail of salts used in biochemistry) with bulk concentration $\rho_\infty = 0.5$ mM. The authors were capable of indirectly measuring the charge density σ_{sample} and the surface potential ψ_{sample}. Note that, within the nomenclature used above, we have $\sigma_{\text{sample}} = -\sigma e_0$ and $\psi_{\text{sample}} = \psi_0$. However, it turns out that the counterions present within the added salt can bind to the PS heads with a dissociation constant $K_d = 1000$ mM, so that only a fraction α of them is available, i.e.

$$\sigma_{\text{sample}} = -\alpha\sigma e_0 \ . \tag{96}$$

Denoting as A_l the membrane area per lipid (assumed to be the same for both PS and PC), within a certain area A we will have $n = A/A_l$ lipids. Of these lipids, $X_{PS} \cdot n = X_{PS}A/A_l$ are charged, so that

$$\sigma = \frac{\frac{X_{PS}A}{A_l}}{A} = \frac{X_{PS}}{A_l} \Rightarrow \sigma_{\text{sample}} = -\alpha\frac{X_{PS}}{A_l}e_0 \ . \tag{97}$$

[6]Reference: Yang, Mayer and Hafner, "Quantitative Membrane Electrostatics with the Atomic Force Microscope", *Biophys. J.* **92**:1966 (2007).

Using Eq.(94), we can thus write

$$\sigma_{\text{sample}} = -\frac{X_{PS} e_0}{A_l \left(1 + \frac{\rho_\infty}{K_d} e^{-\frac{e_0 \psi_0}{k_B T}}\right)} \tag{98}$$

where we set for the bulk concentration of the counterion $[X^+]_\infty = \rho_\infty$, since in this system the counterions come from the salt itself. As mentioned above, the potential can be computed from Grahame's equation, which implies solving the following for ψ_0:

$$\frac{X_{PS}}{A_l \left(1 + \frac{\rho_\infty}{K_d} e^{-\frac{e_0 \psi_0}{k_B T}}\right)} = \sqrt{\frac{2\rho_\infty}{\pi l_B}} \sinh\left(-\frac{e_0 \psi_0}{2 k_B T}\right) \ . \tag{99}$$

In Fig.7, the experimental data are reported alongside Eq.(98) for the charge density (Fig.7a)

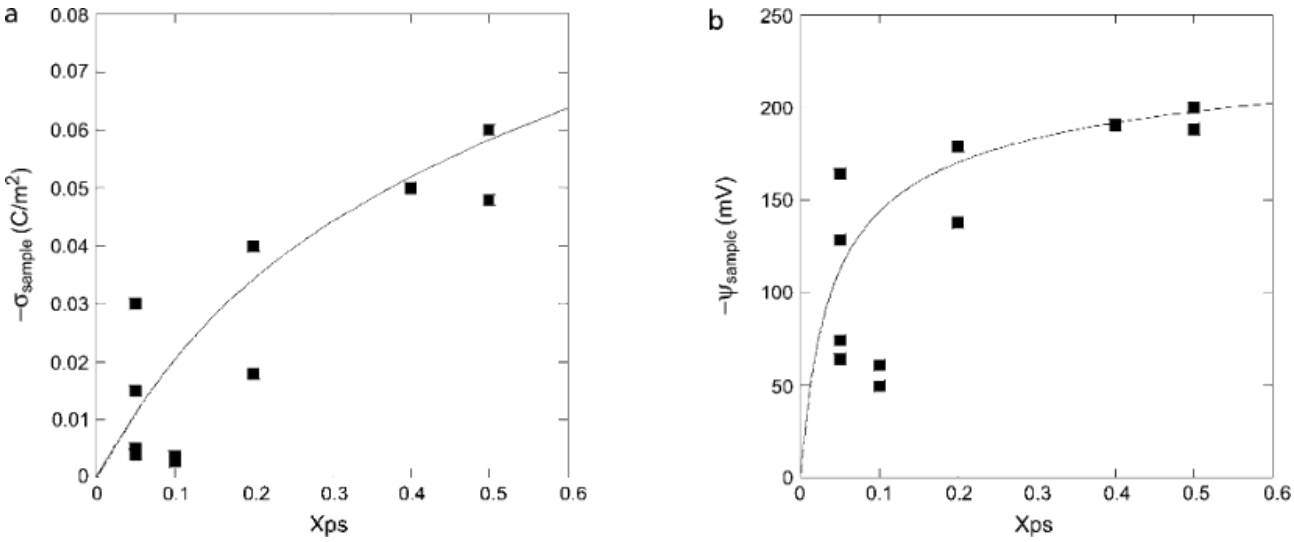

Figure 7: Charge density (a) and potential (b) generated by a membrane with different amounts of PS and PC lipids. Reproduced from Yang, Mayer and Hafner, *Biophys. J.* **92**:1966 (2007).

and the numerical solution of Eq.(99) for the potential (Fig.7b). Note that in spite of the appearances σ_{sample} is not proportional to X_{PS}, since the presence of ψ_0 in the denominator of Eq.(98) introduces a nonlinear dependence on X_{PS} via Eq.(99). Note that the theoretical curves can be used to fit the microscopic parameter A_l, which was found to be equal to $A_l \simeq 0.7$ nm^2.

6 Counterion condensation in cylindrical molecules

We have seen that in a planar geometry most of the counterions are found in the proximity of the surface. As mentioned above, this is easily rationalized observing that the potential generated by a planar surface increases in magnitude linearly with z, i.e. $\psi \propto z$. Hence, at large enough distance the electrostatic attraction between counterions and surface will dominate over their entropy, thus giving rise to the electric double layer.

The situation can be quite different when other geometries are considered. Particularly, in the case of a cylindrical surface of radius r_0 and linear charge density $-\lambda e_0$, the potential generated in the absence of mobile ions is obtained by solving the following Poisson problem

$$\begin{cases} \frac{1}{r}\frac{d}{dr}\left(r\frac{d\psi_c}{dr}\right) = -\frac{-\rho_0 e_0}{\epsilon\epsilon_0} = \frac{\lambda e_0}{\pi r_0^2 \epsilon\epsilon_0} & \text{if } r < r_0 \ , \\ \frac{1}{r}\frac{d}{dr}\left(r\frac{d\psi_d}{dr}\right) = 0 & \text{if } r \geq r_0 \ , \\ \psi_c(r_0) = \psi_d(r_0) \ , \\ \frac{d\psi_c}{dr}(r_0) = \frac{d\psi_d}{dr}(r_0) \ , \\ \frac{d\psi_c}{dr}(0) = 0 \ , \\ \psi_c(r_0) = 0 \ . \end{cases} \tag{100}$$

Indeed, the left-hand side in the differential equations is just $\nabla^2\psi$ in cylindrical coordinates, where the z axis corresponds to the axis of the cylinder. Moreover, assuming a uniformly distributed charge inside the cylinder, if L is the length of the cylinder the total charge is $Q = -\lambda e_0 \cdot L = -\rho_0 \cdot \pi r_0^2 \cdot L \Rightarrow \rho = \lambda/(\pi r_0^2)$. The first two boundary conditions are as before due to the continuity of the potential and of the electric field. The condition $d\psi_c/dr(0) = 0$ stems from the cylindrical symmetry of the problem, which imposes that the electric field is zero along the axis. The last condition, $\psi_c(r_0) = 0$ is simply an arbitrary choice for the zero of the potential at the surface. The differential equations are easily solved by a double integration, yielding

$$\begin{cases} \psi_c(r) = \frac{\lambda e_0}{4\pi\epsilon_0\epsilon r_0^2} r^2 + A_c \ln\frac{r}{r_0} + B_c & \text{if } r < r_0 \ , \\ \psi_d(r) = A_d \ln\frac{r}{r_0} + B_d & \text{if } r \geq r_0 \ , \end{cases} \tag{101}$$

Enforcing the boundary conditions enables computing the integration constants A_c, B_c, A_d, B_d:

$$\begin{cases} A_c = B_d = 0 \ , \\ A_d = \frac{\lambda e_0}{2\pi\epsilon_0\epsilon} \ , \\ B_c = -\frac{\lambda e_0}{4\pi\epsilon_0\epsilon} \ . \end{cases} \tag{102}$$

Summarizing, the potential can thus be written as

$$\psi(r) = \begin{cases} \dfrac{\lambda e_0}{4\pi\epsilon_0\epsilon r_0^2}\left(r^2 - r_0^2\right) & \text{if } z < r_0 \ , \\ \dfrac{\lambda e_0}{2\pi\epsilon_0\epsilon}\ln\dfrac{r}{r_0} & \text{if } r \geq r_0 \ , \end{cases} \tag{103}$$

We see that the potential grows indefinetely with the distance as in the planar case. Nevertheless, the growth here is only logarithmic rather than linear. This feature is key for the odd behavior of counterions in cylindrical geometries. Indeed, let us now consider this object embedded in a liquid in the presence of counterions. We assume that no salt has been added, although the final result can be shown to hold also when salt is present. One could in principle solve the Poisson-Boltzmann equation. Although possible, the derivation is more complex than for the planar case, and goes beyond our present scope. Limiting our consideration to scaling, we note that the electrostatic energy of a cylindrical region of radius r scales as $U_e = \psi \cdot e_0 \sim \lambda e_0^2/(\epsilon_0\epsilon)\ln r \sim k_BT \cdot \lambda l_B \ln r$. The entropic part of the free energy can be estimated starting from the ideal gas, $TS \sim k_BT \ln V$, where $V \sim r^2 L$ is the volume of the cylindrical region. Hence, dropping the term independent of r we can write $TS \sim k_BT \ln r$. At difference with the planar case, here *both* the energy and the entropic term scale as $\ln r$, so that the dominance will be established by the prefactor. Importantly, *only one term dominates at all scales*! This is a striking difference with respect to the planar case, where entropy dominated at small scales and energy at large ones. Now, let us compare the prefactors. The condition under which electrostatics dominates is $U_e > TS \Rightarrow k_BT \cdot \lambda l_B \ln r >\sim k_BT \ln r \Rightarrow \lambda > 1/l_B$. Therefore, it is expected that highly-charged cylindrical molecules will experience a huge collapse of counterions in the vicinity of their surface. This phenomenon is known as *counterion condensation* or *Manning condensation*, and is relevant for many biomolecules, such as DNA.

Based on a more precise calculation, it was shown that the condensation affects a fraction of counterions such that the effective linear charge density becomes $1/l_B$. This makes sense, since an ion far apart from the cylinder will be affected by both the linear charge density on the cylinder and the layer of condensed counterions, so that any further condensation would result in an effective density below the threshold, which would favor entropy over energy. Assuming that no added salt is present, this enables computing the fraction f of condensed counterions. Indeed, if the molecule has length L, then the total number of positive charges on it is $L \cdot \lambda$. Due to electroneutrality, this is also equal to the total number of counterions. If $\lambda > 1/l_B$, Manning condensation takes place until the effective linear density becomes $1/l_B$. Denoting as n_c the number of condensed counterions, we thus have

$$\frac{1}{l_B} = \lambda - \frac{n_c}{L} \Rightarrow n_c = L\left(\lambda - \frac{1}{l_B}\right) \ . \tag{104}$$

The fraction of condensed counterions is thus

$$f = \frac{n_c}{L\lambda} = 1 - \frac{1}{\lambda l_B}. \tag{105}$$

6.1 Example: counterion condensation in DNA

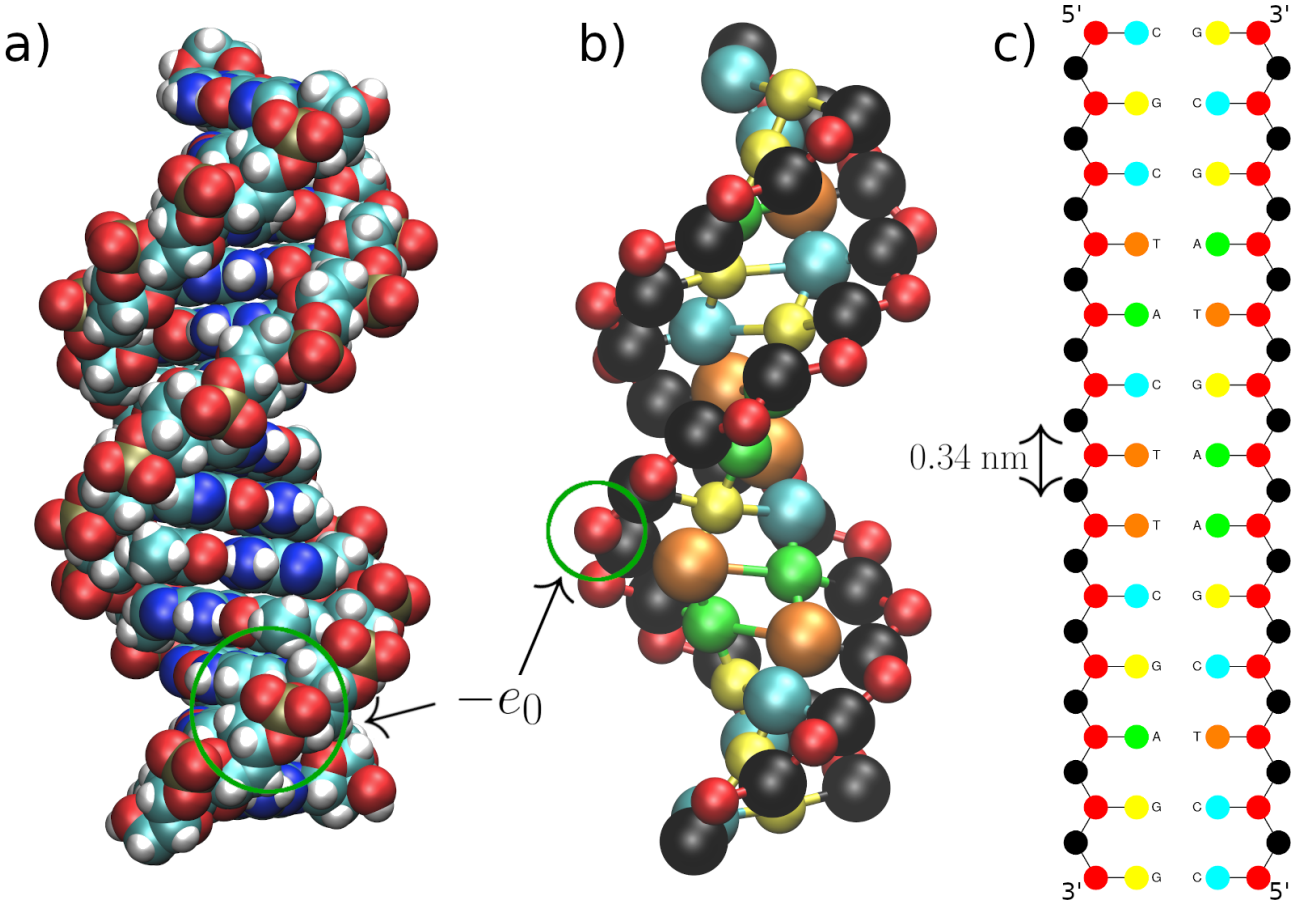

Figure 8: The backbone of DNA has charged phosphate groups (green circles) with distance along the axis roughly equal to 0.34 nm.

An example of counterion condensation is provided by DNA, whose backbone is decorated by negative charges $-e_0$ located on the phosphate groups, as depicted in Fig.8 (green circles). Although simplistic, we will treat here DNA as a simple filament with a certain linear charge density $-\lambda e_0$. As indicated in the figure, the typical distance along the axis between two consecutive phosphates $h \simeq 0.34$ nm (it is called *helical rise* in the DNA literature). A rough estimation of λ can be obtained by observing that there are two charges within a distance h, since there is one charge per strand. Hence, we can estimate $\lambda \simeq 2/h \simeq 5.88$ nm^{-1}. Is it large enough for counterions condensation to take place? In order to answer this question, we need to compare λ with the inverse of the Bjerrum length, $1/l_B \simeq 1/(0.7 \text{ nm}) \simeq 1.43$ nm^{-1}. Since $\lambda > 1/l_B$, we conclude that counterion condensation is indeed to be expected in DNA. From Eq.(105), the fraction of condensed charges is $f = 1 - 1/(\lambda l_B) \simeq 0.76$, i.e. the negative charge

on DNA is so strong that 76% of the counterion condense on its surface! Based on this, one can estimate roughly that DNA behaves as if the phosphates carry a smaller effective charge q. Since counterions condensation takes place in order for the final linear density to be equal to $-e_0/l_B$, we estimate that $-e_0/l_B \simeq 2q/h \Rightarrow q \simeq -he_0/(2l_B) \simeq -0.24e_0$.

Problem. DNA exists also as a single strand, i.e. in Fig.8c only the left or the right chain is present. Its geometry in this case is quite different, and the typical separation between phosphates is roughly $d \simeq 0.44$ nm. Compute the fraction f of condensed counterions and the effective charge of a phosphate group.

7 Interaction between two charged surfaces

7.1 Two planar surfaces

Based on the Gouy-Chapman theory, under certain approximations we can compute the free energy of electrostatic interaction between two planar surfaces. Let us consider two parallel equal surfaces, characterized by a surface density σ of negative charged and put in a solution containing ρ_∞ concentration of monovalent salt. Let the distance between the surfaces be D. Physically, we have a system where the free energy has a contribution coming from the electrostatic potential and an entropic contribution coming from the mobile ions. As for the entropy, we note that the Poisson-Boltzmann equation treats the ions as effectively non-interacting, since they are coupled only via the overall potential $\psi(z)$ (i.e. it is a mean-field theory). In other words, from the entropic point of view the ions can be treated as an ideal gas, for which $pV = Nk_BT \Rightarrow p = \rho k_BT$. Nevertheless, since they have to overcome the pressure exerted by the bulk ions outside of the system, we are interested in the excess pressure

$$p_{\text{entropic}}(z) = [\rho(z) - \rho_\infty]k_BT \ , \tag{106}$$

which is known as *osmotic pressure*. As for the electrostatic part, the pressure exerted at a certain point z between the surfaces can be computed as $p = \text{electrostatic-force}/A$, where A is the area of each surface. The force can be computed as $-dU_e/dz$, where $U_e = (1/2)A\int \epsilon_0\epsilon(d\psi/dz)^2dz$ is the electrostatic energy. The pressure is thus $p = -(1/2)\epsilon_0\epsilon(d\psi/dz)^2$. The sign is negative, meaning that the electrostatic energy is attractive. We thus have

$$p_{\text{enthalpic}}(z) = -\frac{1}{2}\epsilon_0\epsilon\left(\frac{d\psi}{dz}\right)^2 \ . \tag{107}$$

Summing up, considering that we have two species of ions (positive and negative), the pressure at a point z can be written as

$$p(z) = p_{\text{entropic}}(z) + p_{\text{enthalpic}}(z) = [\rho_+(z) - \rho_\infty]k_BT + [\rho_-(z) - \rho_\infty]k_BT - \frac{1}{2}\epsilon_0\epsilon\left(\frac{d\psi}{dz}\right)^2 \ . \tag{108}$$

As we have seen above, for an isolated surface the counterions are strongly localized within a layer of thickness l_D. It is thus expected that for $D \gg l_D$ the potential generated by a surface only slightly perturbs the distribution of counterions in proximity of the other. Based on this, one can used the *Linear Superposition Approximation*, stating that at any point z between the two surfaces the potential is obtained by simply summing the contributions coming from the surfaces as if they were isolated, i.e. by employing Eq.(83). For the present treatment, since $|\gamma| < 1$ we consider the approximate form

$$\psi(z) = -\frac{2k_BT}{e_0}\ln\frac{1-\gamma e^{-\frac{z}{l_D}}}{1+\gamma e^{-\frac{z}{l_D}}} \simeq \frac{4k_BT}{e_0}\gamma e^{-\frac{z}{l_D}} \tag{109}$$

stemming from $\ln((1-x)/(1+x)) \simeq -2x$ valid for $x \ll 1$. We set the origin $z = 0$ at the midpoint, so that the locations of the two surfaces are found at $z = \pm D/2$. For any point z such that $-D/2 \leq z \leq D/2$, the distance from the surface loacted at $-D/2$ is $z + D/2$, while the distance from the other surface is $D/2 - z$. Considering Eq.(109), we can thus write for the potential

$$\psi(z) = \frac{4k_BT}{e_0}\gamma e^{-\frac{z+\frac{D}{2}}{l_D}} + \frac{4k_BT}{e_0}\gamma e^{-\frac{\frac{D}{2}-z}{l_D}} = \frac{4k_BT}{e_0}\gamma e^{-\frac{D}{2l_D}}\left(e^{\frac{z}{l_D}} + e^{-\frac{z}{l_D}}\right) = \frac{8k_BT}{e_0}\gamma e^{-\frac{D}{2l_D}}\cosh\frac{z}{l_D} ,$$

that is, comparing first and last side of the chain of equalities

$$\psi(z) = \frac{8k_BT}{e_0}\gamma e^{-\frac{D}{2l_D}}\cosh\frac{z}{l_D} , \tag{110}$$

Based on this, we can compute the two terms contributing to the pressure. For the entropic part we find:

$$\begin{aligned} & p_{\text{entropic}}(z) = \\ & \left[\rho_+(z) - \rho_\infty\right] k_BT + \left[\rho_-(z) - \rho_\infty\right] k_BT = \\ & \left(\rho_\infty e^{-\frac{e_0\psi}{k_BT}} - \rho_\infty + \rho_\infty e^{\frac{e_0\psi}{k_BT}} - \rho_\infty\right) k_BT = \\ & 2\rho_\infty\left(\cosh\frac{e_0\psi}{k_BT} - 1\right) k_BT = \\ & 4\rho_\infty \sinh^2\frac{e_0\psi}{2k_BT} k_BT , \end{aligned} \tag{111}$$

where we used the identity $\cosh x - 1 = 2\sinh(x/2)$. Assuming that the potential is kept small enough (in line with our observation on $|\gamma| < 1$), we can approximate $\sinh x \simeq x$, thus finding

$$p_{\text{entropic}}(z) \simeq 4\rho_\infty\left(\frac{e_0\psi}{2k_BT}\right)^2 k_BT . \tag{112}$$

Substituting Eq.(110), we finally obtain

$$p_{\text{entropic}}(z) \simeq 4\rho_\infty \cdot 16\gamma^2 e^{-\frac{D}{l_D}}\cosh^2\frac{z}{l_D} \cdot k_BT = 64 k_BT\rho_\infty\gamma^2 e^{-\frac{D}{l_D}}\cosh^2\frac{z}{l_D} . \tag{113}$$

As for the electrostatic part, the derivative of the potential is

$$\frac{d\psi}{dz} = \frac{8k_BT}{e_0}\frac{\gamma}{l_D}e^{-\frac{D}{2l_D}}\sinh\frac{z}{l_D} . \tag{114}$$

Remembering that $l_B = e_0^2/(4\pi\epsilon_0\epsilon)$ and $l_D^2 = 1/(8\pi l_B \rho_\infty)$, we can write for the pressure

$$\begin{aligned} p_{\text{enthalpic}}(z) &= -\frac{1}{2}\epsilon_0\epsilon\left(\frac{d\psi}{dz}\right)^2 = \\ &-\frac{1}{2}\epsilon_0\epsilon\cdot\frac{64(k_BT)^2}{e_0^2}\frac{\gamma^2}{l_D^2}e^{-\frac{D}{l_D}}\sinh^2\frac{z}{l_D} = \\ &-\frac{1}{2}\cdot\frac{64(k_BT)^2}{4\pi l_B k_B T}\cdot\gamma^2\cdot 8\pi l_B\rho_\infty\cdot e^{-\frac{D}{l_D}}\sinh^2\frac{z}{l_D} = \\ &-64k_BT\rho_\infty\gamma^2 e^{-\frac{D}{l_D}}\sinh^2\frac{z}{l_D}\ . \end{aligned} \tag{115}$$

Joining the previous formula and Eq.(113), we obtain for the total pressure $p_D(z)$ at point z with distance D as

$$p_D(z) = 64k_BT\rho_\infty\gamma^2 e^{-\frac{D}{l_D}}\cosh^2\frac{z}{l_D} - 64k_BT\rho_\infty\gamma^2 e^{-\frac{D}{l_D}}\sinh^2\frac{z}{l_D} = 64k_BT\rho_\infty\gamma^2 e^{-\frac{D}{l_D}}\ , \tag{116}$$

which is independent of z, as expected from a system at thermodynamic equilibrium. This pressure is positive, meaning that within the Poisson-Boltzmann theory *two equally-charged surfaces repel each other*. This is by no means trivial, since the electrostatic contribution is actually attractive, i.e. the repulsion comes from the entropy of the mobile ions. It is customary to introduce an interaction constant Z defined as

$$Z \equiv \frac{16k_BT\gamma^2}{l_B} = \frac{64\pi\epsilon_0\epsilon\,(k_BT)^2}{e_0^2}\tanh^2\frac{e_0\psi_0}{4k_BT}\ , \tag{117}$$

which in the case of ions with valence z can be written by operating the substitution $e_0 \to ze_0$ in the denominator. Note that Z depends only on the physico-chemical properties of the surface (and the valence z of the mobile ions), but not on the surface geometry. In this regard, Z plays for electrostatic interactions the same role as the Hamaker constant did for van der Waals interactions. Using Z, the total pressure can be written as

$$p_D = 4\rho_\infty l_B Z e^{-\frac{D}{l_D}}\ . \tag{118}$$

The interaction free energy $F_{\text{plane-plane}}$ can then be obtained from $p = -(\partial F/\partial V)_T$ by integrating over the volume $V = AD$, i.e.

$$F_{\text{plane-plane}}(D) = -\int p_{D'}dV = -A\int_\infty^D p_{D'}dD' = 4\rho_\infty l_B Z A\int_D^\infty e^{-\frac{D'}{l_D}} = 4\rho_\infty l_B Z A l_D e^{-\frac{D}{l_D}}\ .$$

Using the definition $l_D^2 = 1/(8\pi\rho_\infty l_B)$, the previous formula can be rearranged as

$$F_{\text{plane-plane}}(D) = 4\rho_\infty l_B Z A\frac{l_D^2}{l_D}e^{-\frac{D}{l_D}} = 4\rho_\infty l_B Z A\frac{1}{l_D\cdot 8\pi\rho_\infty l_B}e^{-\frac{D}{l_D}} = \frac{ZA}{2\pi l_D}e^{-\frac{D}{l_D}}\ . \tag{119}$$

7.2 Two spherical surfaces

The interaction between two spherical surfaces *with the same charge density* can be estimated by means of the Derjaguin's approximation. We note that the derivation is exactly the same as in the Van der Waals case, so that we can use directly Eq.(80) from the chapter on Van der Waals interactions, obtaining for the magnitude of the total force $f_{\text{sphere-sphere}}$ between the two spheres

$$f_{\text{sphere-sphere}}(D) = 2\pi \frac{R_1 R_2}{R_1 + R_2} \frac{F_{\text{plane-plane}}(D)}{A} = \frac{R_1 R_2}{R_1 + R_2} \frac{Z}{l_D} e^{-\frac{D}{l_D}} \ . \tag{120}$$

As for the free energy, setting the zero at $D = \infty$ one can compute by direct integration (since $f = -dF/dD$) $F_{\text{sphere-sphere}}(D) = F_{\text{sphere-sphere}}(\infty) - \int_\infty^D f_{\text{sphere-sphere}}(D')dD'$, i.e.

$$F_{\text{sphere-sphere}}(D) = \frac{R_1 R_2}{R_1 + R_2} \frac{Z}{l_D} \int_D^\infty e^{-\frac{D'}{l_D}} dD' = \frac{R_1 R_2}{R_1 + R_2} Z e^{-\frac{D}{l_D}} \ . \tag{121}$$

As for the case of the Van der Waals interactions, there is a number of solutions obtained for various geometries, as listed in Fig.9.

Problem. By making use of the Derjaguin's approximation, compute the formula reported in Fig.9 for the case of interaction between a sphere and a planar surface.

7.3 Limit of small potentials

Due to our choice of the zero of the potential $\psi(\infty) = 0$ and since we are considering negatively-charged surfaces, the largest magnitude of ψ is obtained at the surface, where the potential is ψ_0. In the Debye-Hückel limit, $e_0\psi_0/(k_BT) \ll 1$, which corresponds in practice to surface potentials lower than $\simeq 26$ mV.

Problem. For which value of σ is the "thermal" potential $\psi_T = k_BT/e_0$ obtained at the surface? Assuming that we are dealing with a lipid membrane and that one charge per lipid is present, what is the corresponding area per lipid? Ascribing a lipid to a parallelepiped with a square section, what is the length of the side of the section? The headgroups of phospholipids have typical areas ranging between 0.3 and 0.6 nm^2. Can we use the Debye-Hückel approximation safely?

As shown above, the parameter γ corresponds to $\gamma = \tanh(e_0\psi_0/(4k_BT))$, so that in the Debye-Hückel limit $\gamma \ll 1$. The value of γ can be found by solving the equation $\gamma = r - \sqrt{r^2+1}$, where $r = l_{GC}/l_D = \sqrt{2\rho_\infty/(\pi l_B \sigma^2)}$. The limit of small γ is achieved for small σ, i.e. large values of r. Using the approximation $\sqrt{r^2+1} \simeq r + 1/(2r)$ valid for $r \gg 1$, we obtain that for low potentials

$$\gamma \simeq r - \left(r + \frac{1}{2r}\right) = -\frac{1}{2r} = -\sqrt{\frac{\pi l_B \sigma^2}{8\rho_\infty}} \ . \tag{122}$$

Using this result, the interaction constant Z can be written as

$$Z = \frac{16 k_B T \gamma^2}{l_B} \simeq= \frac{16 k_B T}{l_B} \cdot \frac{\pi l_B \sigma^2}{8 \rho_\infty} = \frac{2\pi k_B T \sigma^2}{\rho_\infty} \, . \tag{123}$$

In Fig.10 we show the dependence of Z on the surface density σ (green dashed lines) and compare it to the Debye-Hückel approximation, showing that for the salt concentration chosen (150 mM) the low-potential limit is a reasonable approximation up to $\sigma \simeq 0.1$ nm^{-2}. Note that by construction Z has the units of a force.

Geometry of bodies with surfaces D apart ($D \ll R$)		Electric 'Double-layer' Interaction	
		Energy, W	Force, $F=-dW/dD$
Two ions or small charged molecules	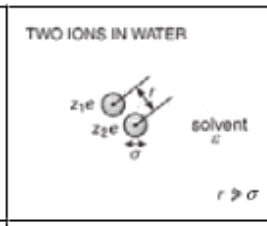	$\frac{+z_1z_2e^2}{4\pi\varepsilon_0\varepsilon r}\frac{e^{-\kappa(r-\sigma)}}{(1+\kappa\sigma)}$	$\frac{+z_1z_2e^2}{4\pi\varepsilon_0\varepsilon r^2}\frac{(1+\kappa r)}{(1+\kappa\sigma)}e^{-\kappa(r-\sigma)}$
Two flat surfaces (per unit area)	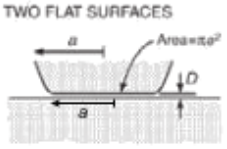	$W_{\text{Flat}} = (\kappa / 2\pi) Ze^{-\kappa D}$	$(\kappa^2 / 2\pi) Ze^{-\kappa D}$
Two spheres or macromolecules of radii R_1 and R_2		$\left(\frac{R_1R_2}{R_1+R_2}\right)Ze^{-\kappa D}$	$\kappa\left(\frac{R_1R_2}{R_1+R_2}\right)Ze^{-\kappa D}$ Also $F = 2\pi\left(\frac{R_1R_2}{R_1+R_2}\right)W_{\text{Flat}}$
Sphere or macromolecule of radius R near a flat surface	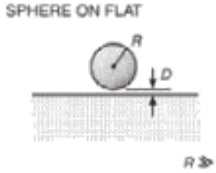	$RZe^{-\kappa D}$	$\kappa RZe^{-\kappa D}$ Also $F = 2\pi R W_{\text{Flat}}$
Two parallel cylinders or rods of radii R_1 and R_2 (per unit length)	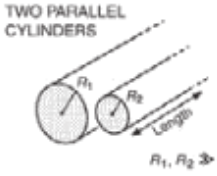	$\frac{\kappa^{-1/2}}{\sqrt{2\pi}}\left(\frac{R_1R_2}{R_1+R_2}\right)^{1/2}Ze^{-\kappa D}$	$\frac{\kappa^{-3/2}}{\sqrt{2\pi}}\left(\frac{R_1R_2}{R_1+R_2}\right)^{1/2}Ze^{-\kappa D}$
Cylinder of radius R near a flat surface (per unit length)	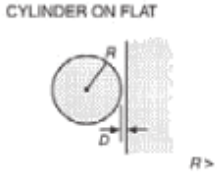	$\kappa^{-1/2}\sqrt{\frac{R}{2\pi}}Ze^{-\kappa D}$	$\kappa^{-3/2}\sqrt{\frac{R}{2\pi}}Ze^{-\kappa D}$
Two cylinders or filaments of radii R_1 and R_2 crossed at 90°	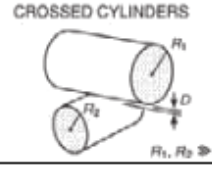	$\sqrt{R_1R_2}Ze^{-\kappa D}$	$\kappa\sqrt{R_1R_2}Ze^{-\kappa D}$ Also $F = 2\pi\sqrt{R_1R_2}W_{\text{Flat}}$

Figure 9: Table listing free energies or free-energy densities for various geometries under the assumptions that the surfaces have the same charge density. Note that also the Debye-Hückel formula has been added for completeness, although here it differs from what we computed since the formula in the table accounts for the small size of the ion. Reprinted from J. N. Israelachvili, "Intermolecular and Surface Forces", 3rd Ed., Academic Press (2011).

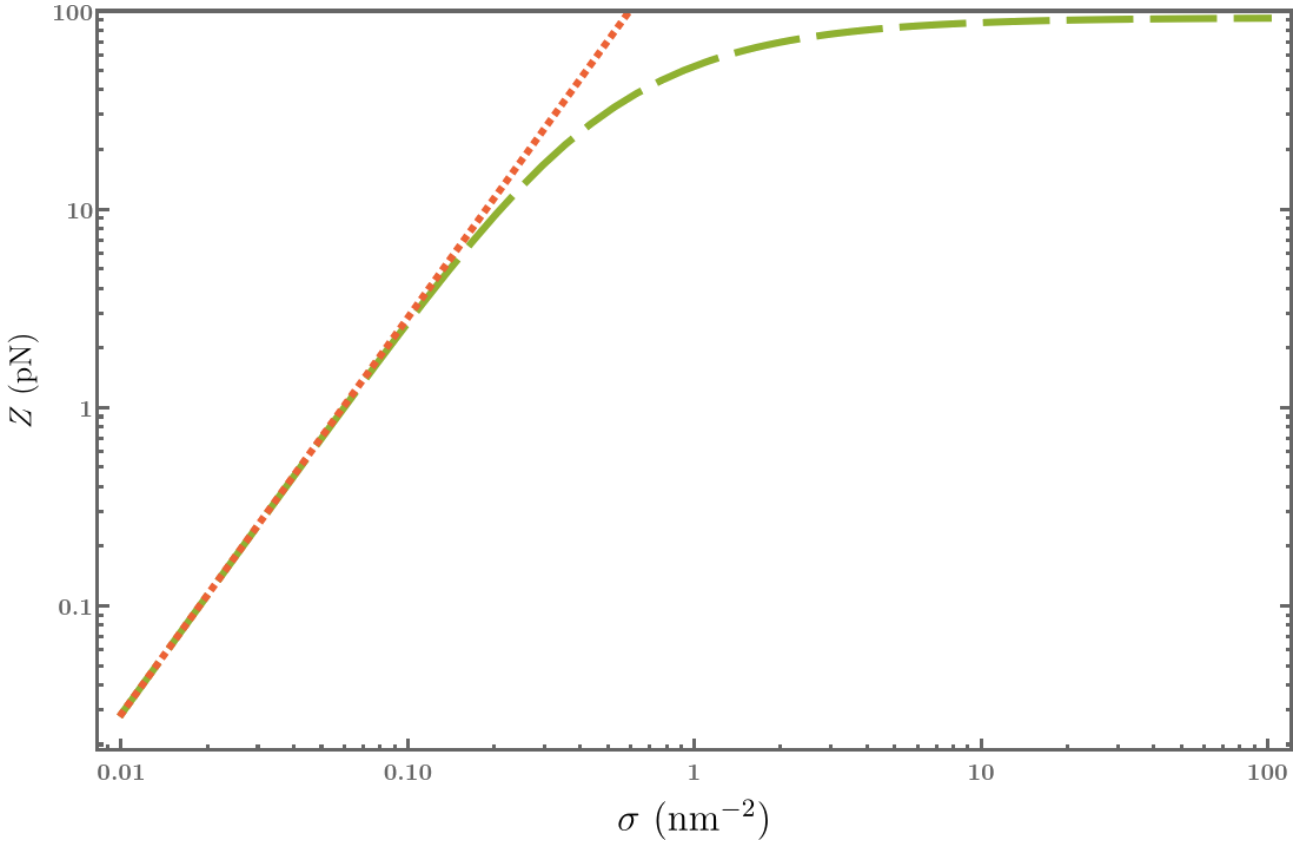

Figure 10: Electrostatic interaction constant as a function of σ for $\rho_\infty = 150$ mM. The green dashed line corresponds to the exact value, while the red dotted line shows the approximation found in the Debye-Hückel limit.

Further reading

- T. Markovich, D. Andelman and R. Podgornik, Charged Membranes: Poisson-Boltzmann theory, DLVO paradigm and beyond, in "Handbook of Lipid Membranes", CRC Press (2021).
- J. N. Israelachvili, "Intermolecular and Surface Forces", 3rd Ed., Academic Press (2011), Chapter 14